```
      WT: yikLFIMIVGGLVGLRIVFAVLSIVnrv
  684+A: yikALFIMIVGGLVGLRIVFAVLSIVnrv
  685+A: yikLAFIMIVGGLVGLRIVFAVLSIVnrv
  686+A: yikLFAIMIVGGLVGLRIVFAVLSIVnrv
  687+A: yikLFIAMIVGGLVGLRIVFAVLSIVnrv
  688+A: yikLFIMAIVGGLVGLRIVFAVLSIVnrv
  689+A: yikLFIMIAVGGLVGLRIVFAVLSIVnrv
  690+A: yikLFIMIVAGGLVGLRIVFAVLSIVnrv
  691+A: yikLFIMIVGAGLVGLRIVFAVLSIVnrv
  692+A: yikLFIMIVGGALVGLRIVFAVLSIVnrv
  693+A: yikLFIMIVGGLAVGLRIVFAVLSIVnrv
  694+A: yikLFIMIVGGLVAGLRIVFAVLSIVnrv
  695+A: yikLFIMIVGGLVGALRIVFAVLSIVnrv
  696+A: yikLFIMIVGGLVGLARIVFAVLSIVnrv
  697+A: yikLFIMIVGGLVGLRAIVFAVLSIVnrv
  698+A: yikLFIMIVGGLVGLRIAVFAVLSIVnrv
  699+A: yikLFIMIVGGLVGLRIVAFAVLSIVnrv
  700+A: yikLFIMIVGGLVGLRIVFAAVLSIVnrv
  702+A: yikLFIMIVGGLVGLRIVFAVALSIVnrv
  703+A: yikLFIMIVGGLVGLRIVFAVLASIVnrv
  704+A: yikLFIMIVGGLVGLRIVFAVLSAIVnrv
  705+A: yikLFIMIVGGLVGLRIVFAVLSIAVnrv
  706+A: yikLFIMIVGGLVGLRIVFAVLSIVAnrv

695+2A: yikLFIMIVGGLVGAALRIVFAVLSIVnrv
695+3A: yikLFIMIVGGLVGAAALRIVFAVLSIVnrv
695+4A: yikLFIMIVGGLVGAAAALRIVFAVLSIVnrv

696+2A: yikLFIMIVGGLVGLAARIVFAVLSIVnrv
695/696+2A: yikLFIMIVGGLVGAALAARIVFAVLSIVnrv
```

Figure 2 Amino acid sequences of the MSD of the wild type (WT) and Ala-insertion mutants used in this study. The predicted MSD portion is indicated in capital letters. The inserted alanine residue is underlined.

observation that mutant gp160, purified from COS-7 cells, is cleaved into the gp120 and gp41 subunits by commercially available Furin *in vitro* (Additional file 1). We also analyzed the trimerization of Env mutants. The trimer of 695+2A Env was detected (Additional file 2) However, the presence of less drastic yet critical structural alterations by the mutation cannot be ruled out completely.

Alanine insertion in the gp41 MSD can alter the intracellular distribution of Env

Since processing of gp160 takes place in the Golgi [7,8], we hypothesized that the defect in the processing was derived from the defect in the intracellular trafficking of mutant Env in the endoplasmic reticulum and Golgi regions. To test this possibility, we examined the distribution of mutant Env in the cells. We attached a FLAG tag at the C-terminus of gp41, providing a linear epitope that can be recognized by monoclonal antibody, M2. An ttachment of the FLAG tag did not alter the defect in processing present in alanine insertion mutants (data not shown). The envelope proteins expressed in COS-7 cells were visualized by immunofluorecent assay using the anti-FLAG monoclonal antibody. We observed that fine, mesh-like fluorescent signals distributing within the transfected cells were more prominent for the mutant 695+2A than the WT (Figure 5). The intensity of fluorescence derived from Env at the Golgi area was notably weaker for 695+2A than for the WT. These data suggested that mutant Env was defective for transport from ER to Golgi. The level of Env expressed on the cell surface, analyzed by FACS, is consistent with this observation because it is lower for the mutant than for the WT (Figure 6).

To further verify the transport defect biochemically, we analyzed the pattern of modification of sugar moieties in the WT and mutant Env. The results are shown in Figure 7. When treated with endoglycosidase H (Endo H), the WT exhibited an Endo H-resistant fraction of gp160 whereas almost no Endo H-resistant gp160 was detected in the 695+2A mutant. This finding indicated that sugar moieties attached to the mutant envelope protein remained as high-mannose types. However, both the WT and mutant envelope proteins generated bands that migrated similarly after treatment with Peptide: N-Glycosidase F (PNGase F), which cleaves between the innermost GlcNAc, and asparagine residues, where sugar moieties are attached. These data further confirmed the defect of the mutant envelope protein in transport, probably in ER-Golgi regions.

The transfer of the gp41 MSD into a foreign membrane protein alters the intracellular distribution of chimeric proteins

We are interested in determining whether the MSD region alone is sufficient to induce the observed transport defect in the context of other membrane proteins. To test this possibility we have replaced the MSD of

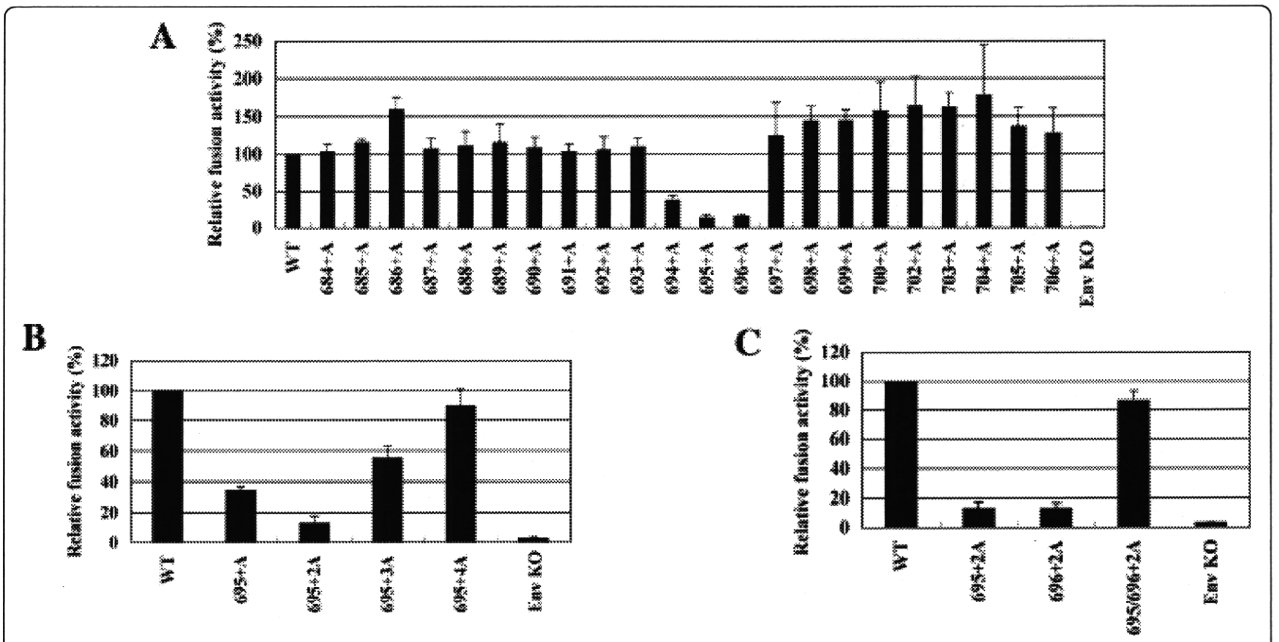

Figure 3 The fusion activity of Ala-insertion mutants in the cell-cell fusion assay. COS-7 cells transfected with the T7 RNA polymerase expression vector and the Env expression vector were co-cultured with 293CD4 cells transfected with a plasmid containing T7 promoter-driven renilla luciferase reporter. After a 24-hr co-culture, the renilla luciferase reporter activity was measured and normalized to the firefly activities as described previously [18]. The normalized renilla luciferase activities for (*A*) single Ala-inserted mutant of Env, (*B*) the mutant Env with multiple Ala insertion, (C) mutant Env with two alanine residues inserted at positions 695 and 696 are shown. Data are the average of three independent experiments. The error bar indicates a standard error.

Tac, the α-chain of the Interleukin-2 receptor, with the MSD of the wild type (Tac-gp41WT) or 695+2A mutant (Tac-gp41+2A) of gp41, and determined the intracellular distribution of the engineered Tac proteins. We included the intact Tac as a reference (Tac-WT). The results are shown in Figure 8. The signals of intact Tac proteins distributed both in the cytoplasm and plasma membrane areas. They show a fine mesh like appearance in the cytoplasm and are well overlapped with the signals of the ER markers. The intact Tac proteins also showed prominent signals at the rim of the cells suggesting efficient transport to the plasma membrane (Figure 8A and 8D). There was no overlap of signals for intact Tac and Golgi markers (Figure 8G). When the MSD of intact Tac proteins was replaced with that of gp41 (wild type in Figure 8B and 8E; 695+2A in C and F), the signals corresponding to the plasma membrane areas became weaker than those of intact Tac (Figure 8, compare A with B and C; D versus E and F). The majority of the signals was observed in the cytoplasm, and the signals were co-localized with ER markers (Figure 8B and 8C). There are some signals of Tac-gp41 chimera in Golgi areas (Figure 8H and 8I). Different from the context of HIV-1 envelope proteins (Figure 5E and 5F), we did not detect a discernable difference in the distribution between the wild type gp41 MSD (Figure 8 Tac-gp41WT) and 695+2A gp41 MSD (Tac-gp41+2A) in the Golgi areas (Figure 8H and 8I). It appeared that the introduction of the gp41 MSD made chimeric Tac distribute in the cytoplasmic region, mainly ER regions, but the difference between the wild type gp41 and 695+2A mutant became less prominent in the context of Tac than in the context of the HIV-1 Env.

Discussion

Although the gp41 MSD has three glycine residues, our CD analysis suggested the presence of the α-helical structure in gp41 MSD (Figure 1). This may not be a surprise, since glycines are abundant in transmembrane helices and glycines are viewed as helix breakers in soluble proteins. A recent molecular dynamics study also supports a helical conformation [30]. Furthermore, the replacement of all three glycine residues with alanine residues, highly α-helix-forming residues [27,28], did not affect the fusion activity of gp41 [18]. Thus gp41 MSD is presumably functional with an α-helical structure. These data, however, do not rule out the possibility of the reported transient alteration of the secondary structure of the gp41 MSD during membrane fusion [11].

Our scanning alanine insertion mutagenesis identified the topological relationship between Gly694 and Arg696 around the MSD α-helix as a critical determinant for the proper processing (Figure 4) and intracellular

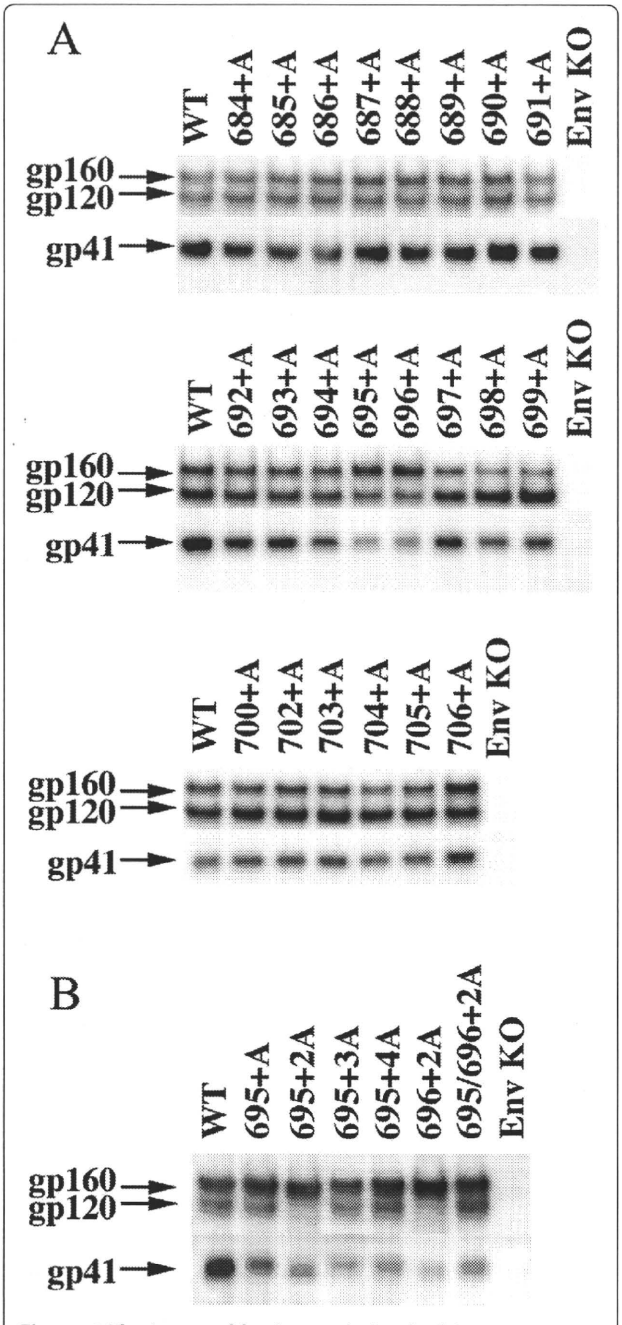

Figure 4 The immunoblotting analysis of wild type (WT) and Ala-inserted mutant Env. The envelope proteins expressed in COS-7 cells transfected with the Env expression vector were detected with anti-gp120 antibody (for gp160 and gp120) or with anti-gp41 antibody. The results of single- and multiple-Ala-insertion mutants are shown in (*A*) and (*B*), respectively.

transport (Figure 5) of Env. Since the processing of gp160 is dependent on the proper transport of the proteins to the Golgi apparatus, it seemed that the observed defect in processing might be due to a transport defect. However, we cannot rule out the possibility of a potential allosteric structural alteration of the Env by mutation in the MSD as a cause for the inefficient processing. Indeed our recent data suggested that the mutations in the gp41 MSD exert allosteric conformational changes of the ectodomain of HIV-1 Env [22].

Mutation at the cleavage site of gp160 eliminates HIV-1 Env fusogenicity [7]. Thus, the defective membrane fusion of our alanine insertion mutants seemed to be derived from improper processing of gp160. However, there are other factors contributing to the defective fusion. Many studies have shown that mutations in the gp41 MSD affect membrane fusion efficiency [18,23,24,29]. In the context of 695+2A mutant, the substitution of hydrophilic arginine residue with non-polar residues (alanine or isoleucine) rescues the defective processing (Additional file 3); however, this could not resolve the defective fusion (Additional file 4). These data suggest that gp41 MSD has a role(s) in the membrane fusion process itself. To reveal the exact mechanism, further studies are required.

It has been reported that MSD length is crucial for the trafficking of membrane proteins [31]. In HIV-1 Env, length of the MSD alone does not seem to be a primary determinant for trafficking. However, our data show that critical information lies in the local structure of the transmembrane α-helix of gp41. It is possible that the alteration of structural features in the MSD region can be sensed by host factor(s) involved in the protein quality control system. This detection could be through the MSD region itself. In a yeast system, some proteins involved in the vesicular transport in ER-Golgi where target recognition was achieved via the MSD region have been reported [32,33]. Since the distribution of our Tac-gp41 chimera was heavily affected by the replacement of the MSD region alone (Figure 8), it may support such a hypothesis. Such a hypothetical factor may recognize wild type gp41 MSD via the GXXXG motif facing outward in relationship to the MSD bundle, if the gp41 MSDs interact with each other through arginine residues as suggested recently [30].

Notably, our alanine insertion mutation altered the relative positioning of the GXXXG motif and arginine residue within the gp41 MSD. Both are major interaction motifs between transmembrane α-helices [34,35]. Although recent electron cryomicroscopic data [36-38] did not provide a spatial arrangement of the gp41 MSD portions, it is possible that there are interactions between the gp41 MSDs during the biosynthesis of the HIV-1 Env. Our alanine insertion may disrupt the interaction among MSDs. This disturbance of interhelical interactions may result in altered intracellular transport. The failure to reproduce differences in intracellular distribution between the wild type and 695+2A MSD, in the context of Tac (Figure 8, B-I), may arise from the

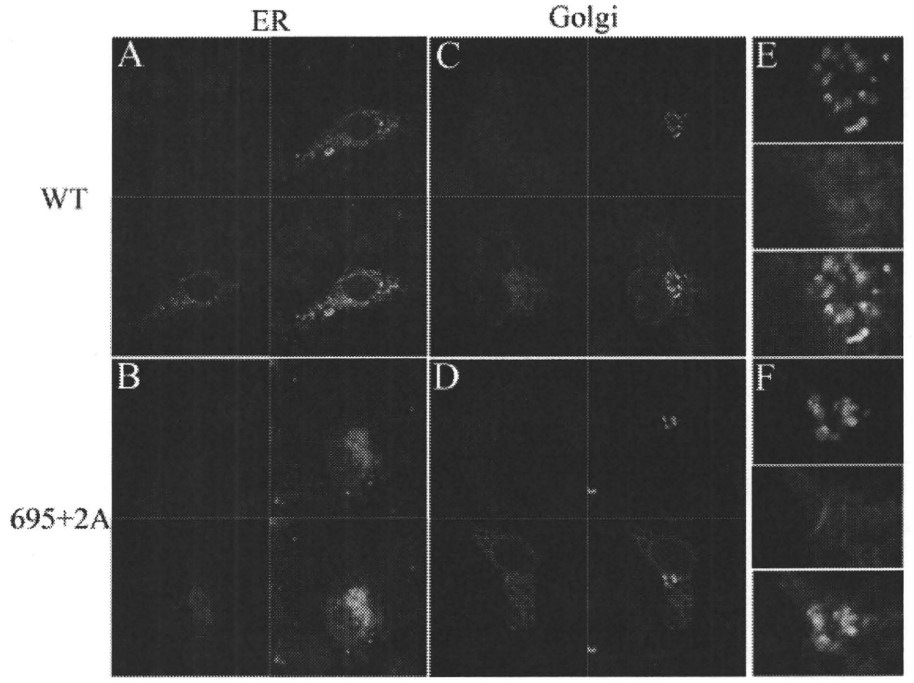

Figure 5 The transport defect of alanine insertion mutant Env. Endoplasmic reticulum (ER) (A and B) and Golgi (C to F) regions were visualized by fluorescence protein-conjugated ER or Golgi marker proteins (shown in green). FLAG tagged WT (A, C and E) and 695+2A Env (B, D and F) were stained by anti-FLAG antibody and Alexa Fluor (shown in red). The close-up of the Golgi area was shown in E and F. Nuclei of cells were stained with Hoechst 33258 (shown in blue).

difference in the oligomeric status between HIV-1 Env (trimer) and Tac (monomer). Our data suggest that mutant Env still forms a trimer (Additional file 2).

Our data clearly demonstrate that the MSD of gp41 has important functions in the biosynthesis of HIV-1 Env, apart from the simple anchoring and modulation of fusion efficiency. The exact regulation mechanism of intracellular distribution of HIV-1 Env by the MSD portion is not known; however, it could be of great importance to determine whether there are any cellular factors that specifically recognize the MSD region of HIV-1 Env.

Conclusions

We have shown that the secondary structure of the synthetic peptide of gp41 MSD is an α-helix. Based on this information, we performed a scanning alanine insertion mutagenesis which showed that alteration of the topological relationship between conserved GXXXG motif and the arginine residue resulted in non-functional Env. The mutant Env manifested a reduced fusion activity and impaired the processing of gp160 into gp120 and gp41. Furthermore, the intracellular transport of mutant Env was affected in the endoplasmic reticulum and Golgi areas. Our data suggested that the specific α-helical structural feature of gp41 MSD controls the biosynthesis of HIV-1 Env.

Methods

Synthesis of MSD peptides and its circular dichroism analysis

The sequence of the peptide used is KKWYIKIFIMIVGGLVGLRIVFAVLSIVNRKK, which corresponds to the consensus sequence of predicted MSD of clade B HIV-1. The sequence of the MSD of the clade B molecular clone, HXB2, used in this study differs by one amino acid from this sequence (indicated by the underline, HXB2 has L instead of I at this position). Two lysine residues were introduced at the N- and C-termini to make the peptide more hydrophilic. The CD spectra were measured at 25°C with Aviv Model 215 (Aviv biomedical Inc, Lakewood, NJ) in 15 mM DPC (n-dodecyl pyridinium chloride), 20 mM NaPi, 150 mM NaCl. The concentration of the peptide was 10 μM. Eight spectra were averaged after subtracting for a DPC reference sample.

Generation of the MSD mutants

QuikChange Site-Directed Mutagenesis kit (Stratagene, La Jolla, CA) generated the mutants used in this study. The plasmid, pGEM7zNB, which contains the 1.2-kb *Nhe*I-*Bam*HI fragment covering the *env* portion of HXB2RU3ΔN, was used as a template as described previously [18]. To facilitate the mutagenesis, silent restriction

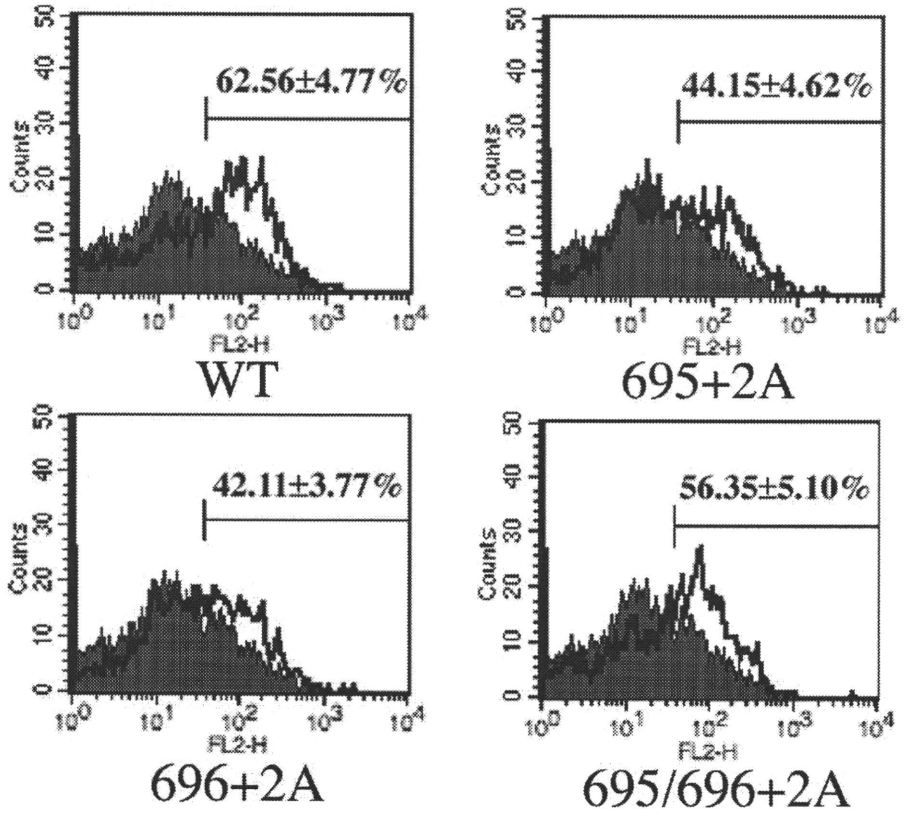

Figure 6 Surface expression level of Env. The cell surface expression level of envelope proteins for WT and Ala-insertion mutants on transfected COS-7 cells was determined by flow cytometry using anti-gp120 antibody.

enzyme sites for *Hind*III, *Spe*I, and *Bsiw*I were generated near the MSD coding region. The complementary oligonucleotide pairs containing an inserted codon, GCC, for the alanine residue were cloned by using the *Hind*III, *Spe*I, and *Bsiw*I sites. Multiple Ala-insertion mutants were made based on the single-insertion mutants. The complementary oligonucleotide pairs used were: 695+A, GGAGGCTTGG TAGGTGCTTT AAGAATAGTT TTT/AAAAACTATT CTTAAAGCAC CTACCAAGCC TCC, 696+A, GGCTTGGTAGGTTTAGCTAGAA-TAGTTTTTGCT/AGCAAAAACTATTCTAGCTAAAC CTACCAAGCC,695+2A,GAGGCTTGGTAGGTGCTG CCTTAAGAATAGTTTTTGC/GCAAAAACTATTCT-TAAGGCAGCACCTACCAAGCCTC,695+3A, GTAG GAGGCTTGGTAGGTGCGGCCGCATTAAGAATAG-TTTTTGCTGTACGTACAGCAAAAACTATTCTTA-ATGCGGCCGCACCTACCAAGCCTCCTAC, 695+4A, GGAGGCTTGGTAGGTGCGGCCGCAGCCTTAA-GAATAGTTT TTGCTGTAC/GTACAGCAAAAAC-TATTCTTAAGGCTGCGGCCGCACCTACCAAGCCT CC,696+2A, GCTTGGTAGGTTTAGCTGCCAGAA-TAGTTTTTGCTG/CAGCAAAAACTATTCTGGCAG CTAAACCTACCAAGC,695/696+2A, GAGGCTTGG-TAGGTGCTGCCTTAGCTGCCAGAATAGTTTTT GCTG/CAGCAAAAACTATTCTGGCAGCTAAGG-CAG CACCTACCAAGCCTC. The *Nhe*I-*BamH*I fragment of pGEM7zNB containing the expected mutations was cloned back to pElucEnv [18] or pElucEnv-3FLAG Env (see below) expression vectors.

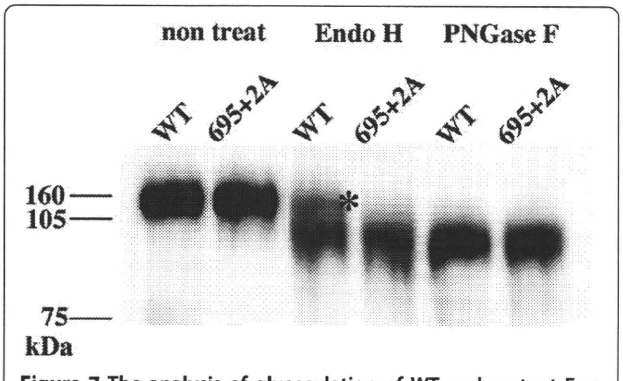

Figure 7 The analysis of glycosylation of WT and mutant Env. The FLAG-tagged Env purified from transfected COS-7 cells was treated with Endo H or PNGase F glycosidase. The treated protein was separated by SDS-PAGE and detected by immunoblotting analysis using anti-FLAG antibody. The asterisk shows the endo H-resistant fraction of Env.

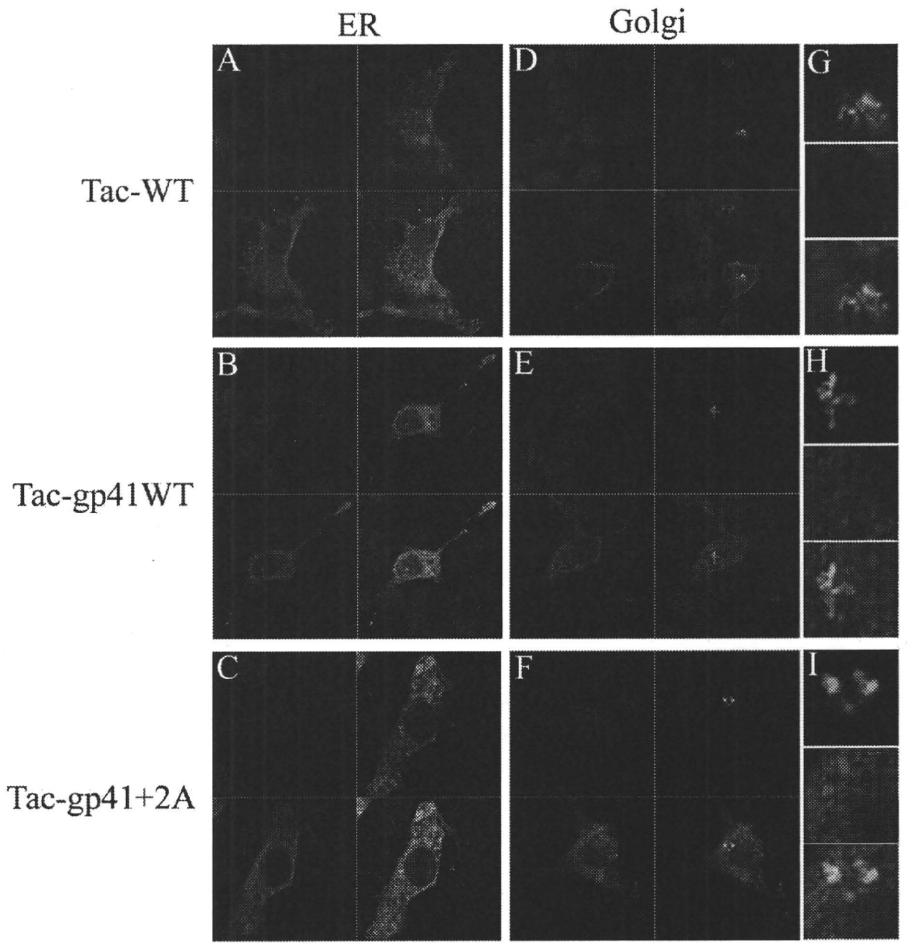

Figure 8 Intracelluar distribution of Tac-gp41MSD chimera. The influence of MSD in transport of Tac proteines. Endoplasmic reticulum (ER) (A to C) and Golgi (D to I) regions were visualized by fluorescence protein-conjugated ER or Golgi marker proteins (shown in green). Halo tagged Tac-WT (A, D and G), Tac-gp41WT (B, E and H) and Tac-gp41 695+2A Env (C, F and I) were stained by anti-Halo antibody, anti-rabbit Ig and Alexa Fluor (shown in red). The close-up of the Golgi area was shown in G to I. Nuclei of cells were stained with Hoechst 33258 (shown in blue).

The synthetic codon-optimized gene corresponding to the Tac protein, α-chain of Interleukin-2 receptor, with the gp41 MSD was custom synthesized (GenScript, Piscataway, NJ). The derivatives of this construct, whose MSD portion was replaced with those of wild type or mutant gp41 or intact Tac, were generated by mutagenesis using PCR. These genes were cloned downstream of the CMV promoter to generate the Tac-derivative expression vectors.

Addition of the 3 × FLAG tag at the C-terminus of the Env

A 3 × FLAG tag was added to the C-terminus of gp41 by inserting oligonucleotides corresponding to the 3 × FLAG tag sequence derived from the vector p3xFLAG-CMV™-7.1 (Sigma, St. Louis, MO). Following this insertion, the amino acid sequence after the C-terminus of gp41 reads as RSARDYKDHDGDYKDHDIDYKDDDDK. The expression vector of FLAG-tagged Env was called pElucEnv-3FLAG Env.

Cells and antibodies

COS-7 cells, 293 cells, and 293-CD4 cells [18] were grown in Dulbecco's modified Eagle's medium (Sigma, St. Louis, MO) supplemented with 10% fetal bovine serum (HyClone Laboratories, Logan, UT) and penicillin-streptomycin (Invitrogen, Carlsbad, CA). Cells were kept under 5% CO_2 in a humidified incubator. Anti-gp120 polyclonal antibody was obtained from Fitzgerald Industries International, Inc. (Concord, MA). The hybridoma 902 and Chessie 8 were obtained from Bruce Chesebro and George Lewis, respectively through the AIDS Research and Reference Reagent Program, Division of AIDS, National Institute of Allergy and Infectious

Diseases, National Institutes of Health, USA [39-41]. Anti-FLAG M2 and BioM2 were purchased from Sigma (St Louis, MO).

Cell-cell fusion assay

Cell-cell fusion assays, using T7 RNA polymerase (T7 RNA pol) transfer, were performed as described previously [18]. Briefly, 293-CD4 cells that constitutively express CD4 were transfected with pTM3hRL harboring the T7 promoter-driven renilla luciferase gene by FuGene 6 (Roche Applied Science, Mannheim, Germany), and were co-cultured with COS-7 cells that had been transfected with pCMMPT7iresGFP, a T7 RNA polymerase expression vector, and pElucEnv containing HIV-1 Env and firefly luciferase genes by FuGene 6. After 12 hours of co-culture, the renilla and firefly luciferase activities were measured using the Dual-Glo luciferase assay system (Promega, Madison, WI). The fusion activity, represented by renilla luciferase activity, was normalized by firefly luciferase activity to obtain transfection efficiency [18]. The polyclonal anti-halo antibody was obtained from Promega (Promega, Madison, WI).

Immunoblotting analysis

5×10^4 COS-7 cells were transfected with pElucEnv by FuGene 6 in a 24-well culture plate. Forty-eight hours after transfection, the cells were lysed with radioimmunoprecipitation assay lysis buffer (0.05 M TrisCl, 0.15 M NaCl, 1% Triton X-100, 0.1% sodium dodecyl sulfate, and 1% sodium deoxycholate). Cell lysates were electrophoresed (5-20% Pantera Gel, DRC, Tokyo, Japan) and transferred to a polyvinylidene fluoride membrane (Pall, East Hills, NY). The blot was probed with anti-gp120 antibody (Fitzgerald, Concord, MA), with the monoclonal anti-gp41 antibody (Chessie 8), or with anti-FLAG M2 antibody. A biotinylated anti-species-specific immunoglobulin (GE Healthcare Bio-Sciences AB, Uppsala, Sweden) was used as the secondary antibody. The blot was further treated with a streptavidin-horseradish peroxidase conjugate (GE Healthcare Bio-Sciences AB) and Lumi-Light^{plus} (Roche, Indianapolis, IN). Images were obtained with LAS3000 (Fujifilm, Tokyo, Japan).

Immunofluorescence assay

Immunofluorescence assays were used to determine the intracellular distribution of the envelope proteins. For this purpose, we generated a modified envelope expression vector called pElucEnvdeltaGFP; this is the derivative of the previously described pElucEnv [18] and it has the deletion of the EGFP portion. COS-7 cells transfected with pElucEnv WT or 695+2A in the delta GFP backbone vector and ER-DsRed2 or Golgi-YPF (Clontech) or pER-mAG1 (MBL, Nagoya, Japan) plasmid by FuGene 6 (Roche) were treated with PBS including 4% of PFA for 5 min at 48 hr posttransfection. Cells were permeabilized by PBS including, 0.05% of saponin and 0.2% of BSA, for 30 min and then stained with 20 μg/ml of bio-M2 (Sigma) antibody and 10 μg/ml of streptavidin conjugated Alexa fluor 488 or 555 (Invitrogen). In the case of Halo-tagged proteins, polyclonal anti-Halo antibodies were used as primary antibodies. The distributions of fluorescence in cells were visualized using a Zeiss LSM 510 meta confocal microscope.

Flow cytometric analysis

Flow cytometric analysis was performed as described previously [18]. Briefly, COS-7 cells were transfected with pElucEnv by FuGene 6 on a six-well plate. Forty-eight hours aftertransfection, the cells were stained with anti-gp120 monoclonal antibody 902, biotinXX anti-mouse IgG (Invitrogen) and streptavidin-Alexa 555 in PBS including 10% FBS. Cells were fixed with 1% paraformaldehyde in PBS and analyzed by FACS Calibur (BD Biosciences).

Glycosidase assay

COS-7 cells transfected with pElucEnv-3FLAG by FuGene 6 on the six-well plate were lysed with radioimmunoprecipitation assay lysis buffer including Complete protease inhibitor (Roche). Env-3FLAG was purified from cell lysates by immunoprecipitation using M2 agarose (Sigma) and eluted with 3XFLAG peptide (Sigma). Purified Env-3FLAG was treated with Endo H or PNGase F (Roche). For digestion by Endo H, Env-3FLAG was boiled and digested with 0.005 unit Endo H at 37°C for 12 hr in Endo H digestion buffer [50 mM phosphate buffer (pH 5.8), 50 mM NaCl, 0.1 M 2-mercaptoethanol (2-ME), 0.01% SDS]. Env-3FLAG was boiled in PBS including 0.1 M 2-ME and 0.1% SDS and digested by 1 unit PNGase F at 37°C for 12 hr in PNGase F digestion buffer (74 mM TrisCl, pH 8.0; 0.74% NP-40; 0.37 M 2-ME, 0.37% SDS). Env-3FLAG treated with glycosidase was resolved by SDS-polyacrylamide gel electrophoresis (10% polyacrylamide gel; DRC) and detected by immunoblotting analysis using anti-FLAG M2.

In vitro furin cleavage of Env

Env-3FLAG with the 695+2A mutation was purified from COS-7 cell lysates by immunoprecipitation as described above and treated with 0.7 units of furin (Alexis, Lausen, Switzerland) at 30°C for 12 hr in furin-digestion buffer (100 mM Hepes, pH 7.5; 1 mM $CaCl_2$; 0.5% Triton X-100]). Env-3FLAG, treated with furin, was detected by immunoblotting analysis using anti-FLAG M2 as described above.

The cross linking analysis of Env

At 48 hr postransfection, 293T cells transfected with FLAG tagged WT or 695+2A Env expression vectors were treated with 1 mM DSS for 20 min at room temperature in PBS (pH 8.0). Cells were incubated with 20 mM Tris-Cl for 15 min at room temperature to stop the reaction and then were lysed in buffer A (10 mM HEPES, 1.5 mM MgCl2, 10 mM KCl, 0.5 mM DTT, 0.05% Igepal pH 7.9). Env proteins in cellular lysate were detected by immunoblotting analysis using anti-FLAG antibody (see above).

Additional material

Additional file 1: Supplemental Figure 1- In vitro digestion of mutant Env with recombinant Furin. The wild type (WT) and mutant (695+2A) Env were prepared from transfected COS-7 cells and subjected to digestion with recombinant Furin (rFurin) as described in the Methods section. Mock indicates the result for the cell lysates prepared from mock transfected cells.

Additional file 2: Suplemental Figure 2- Cross linking analysis of the 695+2A Env. The trimerization of gp160 was examined by chemical cross linking. The cells transfected with Env expression vectors for wild type (WT) and mutant (695+2A) were treated with the chemical cross linker. The cell lysates were probed with the anti-FLAG antibody. The single asterisk and the double asterisk indicate the bands for trimer and monomer of mutant gp160, respectively. Marker: HiMark Pre-Stained High Molecular Weight Protein Standard (Invitrogen), Mock: mock transfection.

Additional file 3: Suplemental Figure 3A - Immunoblotting analysis of the Arg-substitution mutants in the context of 695+2A. The degree of processing of gp160 was examined by immunoblotting the cell lysates prepared from COS-7 cells transfected with respective Env expression vectors. The Arg residue in the context of 695+2A was substituted with the indicated amino acid residue by the site directed mutagenesis (columns under 2A). One letter abbreviation for an amino acid residue is used. Mock: mock transfection, WT: wild type MSD.

Additional file 4: Suplemental Figure 3B - Fusion activities of Arg-substitution mutants in the context of 695+2A. The fusion activities of the mutant shown in additional file 3A were examined by a syncytia formation assay in 293CD4 cells. Fusion activity of the WT and MSD mutants was expressed using a fusion index (fusion index = 2x + y, where x is the number of multinucleated cells [number of nuclei ≥ 5 in five visual fields] and y is the number of multinucleated cells [number of nuclei < 5 in five visual fields]) as described previously [18].

List of abbreviations

MSD: membrane-spanning domain; CD: circular dichroism; ER: endoplasmic reticulum; WT: wild type.

Acknowledgements

This study was supported by a contract grant from the Ministry of Education, Culture, Sports, Science and Technology of Japan for the Program of Founding Research Centers for Emerging and Reemerging Infectious Diseases and a grant from the USNIH to DME (GM073857). We thank Dr. Kunito Yoshiike for his critical reading of the manuscript. We thank A. M. Menting, an editorial consultant, for help in the preparation of the manuscript.

Author details

[1]Laboratory of Virology and Pathogenesis, AIDS Research Center, National Institute of Infectious Diseases, 1-23-1 Toyama, Shinjuku, Tokyo, Japan. [2]Department of Molecular Biophysics and Biochemistry, Yale University, Box 208114, New Haven, CT 06520-8114, USA. [3]China-Japan Joint Laboratory of Structural Virology and Immunology, Institute of Biophysics, Chinese Academy of Sciences, 15 Datun Road, Beijing, 100101 PR China. [4]Division of Infectious Diseases, Advanced Clinical Research Center, University of Tokyo, 4-6-1 Shirokanedai, Minato-ku, Tokyo, Japan. [5]Research Center for Asian Infectious Diseases, Institute of Medical Science, University of Tokyo, 4-6-1 Shirokanedai, Minato-ku, Tokyo, Japan. [6]*Current Address:* Department of Pediatrics, Emory University School of Medicine, 2015 uppergate Dr. Atlanta, GA 30322, USA.

Authors' contributions

KM, ARC, YL and **NK** performed most of the experimental work. **KM, YL** and **NK** did the cell biological analyses of mutant Envs. ARC analysed the synthetic peptide for its biophysical properties. **AI** contributed to discussion. **DME** and **ZM** conceived the study and coordinated the experiments. All authors read and approved the final manuscript.

Competing interests

The authors declare that they have no competing interests.

Received: 14 July 2010 Accepted: 13 November 2010
Published: 13 November 2010

References

1. Weiss CD: **HIV-1 gp41: mediator of fusion and target for inhibition.** *AIDS Rev* 2003, **5**:214-221.
2. Eckert DM, Kim PS: **Mechanisms of viral membrane fusion and its inhibition.** *Annu Rev Biochem* 2001, **70**:777-810.
3. Freed EO, Martin MA: **The role of human immunodeficiency virus type 1 envelope glycoproteins in virus infection.** *J Biol Chem* 1995, **270**:23883-23886.
4. Gu M, Rappaport J, Leppla SH: **Furin is important but not essential for the proteolytic maturation of gp160 of HIV-1.** *FEBS Lett* 1995, **365**:95-97.
5. Moulard M, Decroly E: **Maturation of HIV envelope glycoprotein precursors by cellular endoproteases.** *Biochim Biophys Acta* 2000, **1469**:121-132.
6. Ohnishi Y, Shioda T, Nakayama K, Iwata S, Gotoh B, Hamaguchi M, Nagai Y: **A furin-defective cell line is able to process correctly the gp160 of human immunodeficiency virus type 1.** *J Virol* 1994, **68**:4075-4079.
7. McCune JM, Rabin LB, Feinberg MB, Lieberman M, Kosek JC, Reyes GR, Weissman IL: **Endoproteolytic cleavage of gp160 is required for the activation of human immunodeficiency virus.** *Cell* 1988, **53**:55-67.
8. Kantanen ML, Leinikki P, Kuismanen E: **Endoproteolytic cleavage of HIV-1 gp160 envelope precursor occurs after exit from the trans-Golgi network (TGN).** *Arch Virol* 1995, **140**:1441-1449.
9. Gabuzda D, Olshevsky U, Bertani P, Haseltine WA, Sodroski J: **Identification of membrane anchorage domains of the HIV-1 gp160 envelope glycoprotein precursor.** *J Acquir Immune Defic Syndr* 1991, **4**:34-40.
10. Dimmock NJ: **The complex antigenicity of a small external region of the C-terminal tail of the HIV-1 gp41 envelope protein: a lesson in epitope analysis.** *Rev Med Virol* 2005, **15**:365-381.
11. Lu L, Zhu Y, Huang J, Chen X, Yang H, Jiang S, Chen YH: **Surface exposure of the HIV-1 env cytoplasmic tail LLP2 domain during the membrane fusion process: interaction with gp41 fusion core.** *J Biol Chem* 2008, **283**:16723-16731.
12. Haffar OK, Dowbenko DJ, Berman PW: **Topogenic analysis of the human immunodeficiency virus type 1 envelope glycoprotein, gp160, in microsomal membranes.** *J Cell Biol* 1988, **107**:1677-1687.
13. Helseth E, Olshevsky U, Gabuzda D, Ardman B, Haseltine W, Sodroski J: **Changes in the transmembrane region of the human immunodeficiency virus type 1 gp41 envelope glycoprotein affect membrane fusion.** *J Virol* 1990, **64**:6314-6318.
14. Yue L, Shang L, Hunter E: **Truncation of the membrane-spanning domain of human immunodeficiency virus type 1 envelope glycoprotein defines elements required for fusion, incorporation, and infectivity.** *J Virol* 2009, **83**:11588-11598.
15. West JT, Johnston PB, Dubay SR, Hunter E: **Mutations within the putative membrane-spanning domain of the simian immunodeficiency virus transmembrane glycoprotein define the minimal requirements for fusion, incorporation, and infectivity.** *J Virol* 2001, **75**:9601-9612.

16. Senes A, Engel DE, DeGrado WF: **Folding of helical membrane proteins: the role of polar, GxxxG-like and proline motifs.** *Curr Opin Struct Biol* 2004, **14**:465-479.
17. Wilk T, Pfeiffer T, Bukovsky A, Moldenhauer G, Bosch V: **Glycoprotein incorporation and HIV-1 infectivity despite exchange of the gp160 membrane-spanning domain.** *Virology* 1996, **218**:269-274.
18. Miyauchi K, Komano J, Yokomaku Y, Sugiura W, Yamamoto N, Matsuda Z: **Role of the specific amino acid sequence of the membrane-spanning domain of human immunodeficiency virus type 1 in membrane fusion.** *J Virol* 2005, **79**:4720-4729.
19. Deml L, Kratochwil G, Osterrieder N, Knuchel R, Wolf H, Wagner R: **Increased incorporation of chimeric human immunodeficiency virus type 1 gp120 proteins into Pr55gag virus-like particles by an Epstein-Barr virus gp220/350-derived transmembrane domain.** *Virology* 1997, **235**:10-25.
20. Salzwedel K, Johnston PB, Roberts SJ, Dubay JW, Hunter E: **Expression and characterization of glycophospholipid-anchored human immunodeficiency virus type 1 envelope glycoproteins.** *J Virol* 1993, **67**:5279-5288.
21. Owens RJ, Burke C, Rose JK: **Mutations in the membrane-spanning domain of the human immunodeficiency virus envelope glycoprotein that affect fusion activity.** *J Virol* 1994, **68**:570-574.
22. Kondo N, Miyauchi K, Meng F, Iwamoto A, Matsuda Z: **Conformational changes of the HIV-1 envelope protein during membrane fusion were inhibited by the replacement of its membrane-spanning domain.** *J Biol Chem* 2010, **285**:14681-8.
23. Miyauchi K, Curran R, Matthews E, Komano J, Hoshino T, Engelman DM, Matsuda Z: **Mutations of conserved glycine residues within the membrane-spanning domain of human immunodeficiency virus type 1 gp41 can inhibit membrane fusion and incorporation of Env onto virions.** *Jpn J Infect Dis* 2006, **59**:77-84.
24. Shang L, Yue L, Hunter E: **Role of the membrane-spanning domain of human immunodeficiency virus type 1 envelope glycoprotein in cell-cell fusion and virus infection.** *J Virol* 2008, **82**:5417-5428.
25. Ratner L, Fisher A, Jagodzinski LL, Liou RS, Mitsuya H, Gallo RC, Wong-Staal F: **Complete nucleotide sequences of functional clones of the virus associated with the acquired immunodeficiency syndrome, HTLV-III/LAV.** *Haematol Blood Transfus* 1987, **31**:404-406.
26. Andreassen H, Bohr H, Bohr J, Brunak S, Bugge T, Cotterill RM, Jacobsen C, Kusk P, Lautrup B, Petersen SB, *et al*: **Analysis of the secondary structure of the human immunodeficiency virus (HIV) proteins p17, gp120, and gp41 by computer modeling based on neural network methods.** *J Acquir Immune Defic Syndr* 1990, **3**:615-622.
27. Pace CN, Scholtz JM: **A helix propensity scale based on experimental studies of peptides and proteins.** *Biophys J* 1998, **75**:422-427.
28. Chakrabartty A, Schellman JA, Baldwin RL: **Large differences in the helix propensities of alanine and glycine.** *Nature* 1991, **351**:586-588.
29. Welman M, Lemay G, Cohen EA: **Role of envelope processing and gp41 membrane spanning domain in the formation of human immunodeficiency virus type 1 (HIV-1) fusion-competent envelope glycoprotein complex.** *Virus Res* 2007, **124**:103-112.
30. Kim JH, Hartley TL, Curran AR, Engelman DM: **Molecular dynamics studies of the transmembrane domain of gp41 from HIV-1.** *Biochim Biophys Acta* 2009, **1788**:1804-1812.
31. Ronchi P, Colombo S, Francolini M, Borgese N: **Transmembrane domain-dependent partitioning of membrane proteins within the endoplasmic reticulum.** *J Cell Biol* 2008, **181**:105-118.
32. Sato K, Sato M, Nakano A: **Rer1p, a retrieval receptor for ER membrane proteins, recognizes transmembrane domains in multiple modes.** *Mol Biol Cell* 2003, **14**:3605-3616.
33. Reggiori F, Black MW, Pelham HR: **Polar transmembrane domains target proteins to the interior of the yeast vacuole.** *Mol Biol Cell* 2000, **11**:3737-3749.
34. Curran AR, Engelman DM: **Sequence motifs, polar interactions and conformational changes in helical membrane proteins.** *Curr Opin Struct Biol* 2003, **13**:412-417.
35. Cosson P, Lankford SP, Bonifacino JS, Klausner RD: **Membrane protein association by potential intramembrane charge pairs.** *Nature* 1991, **351**:414-416.
36. Zhu P, Liu J, Bess J, Chertova E, Lifson JD, Grise H, Ofek GA, Taylor KA, Roux KH: **Distribution and three-dimensional structure of AIDS virus envelope spikes.** *Nature* 2006, **441**:847-852.
37. Liu J, Bartesaghi A, Borgnia MJ, Sapiro G, Subramaniam S: **Molecular architecture of native HIV-1 gp120 trimers.** *Nature* 2008, **455**:109-113.
38. Zhu P, Winkler H, Chertova E, Taylor KA, Roux KH: **Cryoelectron tomography of HIV-1 envelope spikes: further evidence for tripod-like legs.** *PLoS Pathog* 2008, **4**:e1000203.
39. Chesebro B, Wehrly K: **Development of a sensitive quantitative focal assay for human immunodeficiency virus infectivity.** *J Virol* 1988, **62**:3779-3788.
40. Pincus SH, Wehrly K, Chesebro B: **Treatment of HIV tissue culture infection with monoclonal antibody-ricin A chain conjugates.** *J Immunol* 1989, **142**:3070-3075.
41. Abacioglu YH, Fouts TR, Laman JD, Claassen E, Pincus SH, Moore JP, Roby CA, Kamin-Lewis R, Lewis GK: **Epitope mapping and topology of baculovirus-expressed HIV-1 gp160 determined with a panel of murine monoclonal antibodies.** *AIDS Res Hum Retroviruses* 1994, **10**:371-381.

doi:10.1186/1742-4690-7-95
Cite this article as: Miyauchi *et al.*: **The membrane-spanning domain of gp41 plays a critical role in intracellular trafficking of the HIV envelope protein.** *Retrovirology* 2010 **7**:95.

RETROVIROLOGY

RESEARCH Open Access

Membrane topology analysis of HIV-1 envelope glycoprotein gp41

Shujun Liu[1†], Naoyuki Kondo[1,2,3†], Yufei Long[1], Dan Xiao[1], Aikichi Iwamoto[3], Zene Matsuda[1,2*]

Abstract

Background: The gp41 subunit of the HIV-1 envelope glycoprotein (Env) has been widely regarded as a type I transmembrane protein with a single membrane-spanning domain (MSD). An alternative topology model suggested multiple MSDs. The major discrepancy between the two models is that the cytoplasmic Kennedy sequence in the single MSD model is assigned as the extracellular loop accessible to neutralizing antibodies in the other model. We examined the membrane topology of the gp41 subunit in both prokaryotic and mammalian systems. We attached topological markers to the C-termini of serially truncated gp41. In the prokaryotic system, we utilized a green fluorescent protein (GFP) that is only active in the cytoplasm. The tag protein (HaloTag) and a membrane-impermeable ligand specific to HaloTag was used in the mammalian system.

Results: In the absence of membrane fusion, both the prokaryotic and mammalian systems (293FT cells) supported the single MSD model. In the presence of membrane fusion in mammalian cells (293CD4 cells), the data obtained seem to support the multiple MSD model. However, the region predicted to be a potential MSD is the highly hydrophilic Kennedy sequence and is least likely to become a MSD based on several algorithms. Further analysis revealed the induction of membrane permeability during membrane fusion, allowing the membrane-impermeable ligand and antibodies to cross the membrane. Therefore, we cannot completely rule out the possible artifacts. Addition of membrane fusion inhibitors or alterations of the MSD sequence decreased the induction of membrane permeability.

Conclusions: It is likely that a single MSD model for HIV-1 gp41 holds true even in the presence of membrane fusion. The degree of the augmentation of membrane permeability we observed was dependent on the membrane fusion and sequence of the MSD.

Background

The envelope glycoprotein (Env) of human immunodeficiency virus type-1 (HIV-1) plays a critical role in the early stage of HIV-1 infection. Env is synthesized as a precursor protein, gp160 [1,2], and processed into gp120 and gp41 during transport from the endoplasmic reticulum to Golgi network [3,4]. The gp120 subunit determines host range through its recognition of the receptor and co-receptor complex. The transmembrane protein gp41 mediates the membrane fusion between the host and viral membranes. It is composed of an ectodomain (extracellular domain), a cytoplasmic domain, and a transmembrane domain. The ectodomain has coiled-coil-forming heptad repeats essential for membrane fusion. The cytoplasmic domain contains three amphipathic helices called the lentiviral lytic peptide (LLP) 1, 2 and 3. The LLP-1 and LLP-2 portions have a high hydrophobic moment common to membrane-lytic peptides [5-9].

The transmembrane domain of gp41 was first deduced from the hydropathy plot of Env as a hydrophobic domain [10]. This transmembrane domain, herein referred to as the membrane-spanning domain (MSD), is composed of 23 highly conserved amino acid residues corresponding to amino acid residues 684 to 706 in the HXB2 strain (Figure 1A, B). An in vitro translation study in the presence of microsomal membranes suggested that HIV-1 Env has one MSD [11], as predicted by the hydropathy plot. In that study, the C-terminus of

* Correspondence: zmatsuda@ims.u-tokyo.ac.jp
† Contributed equally
[1]China-Japan Joint Laboratory of Structural Virology and Immunology, Institute of Biophysics, Chinese Academy of Sciences, 15 Datun Road, Chaoyang District, Beijing 100101, P. R. China
Full list of author information is available at the end of the article

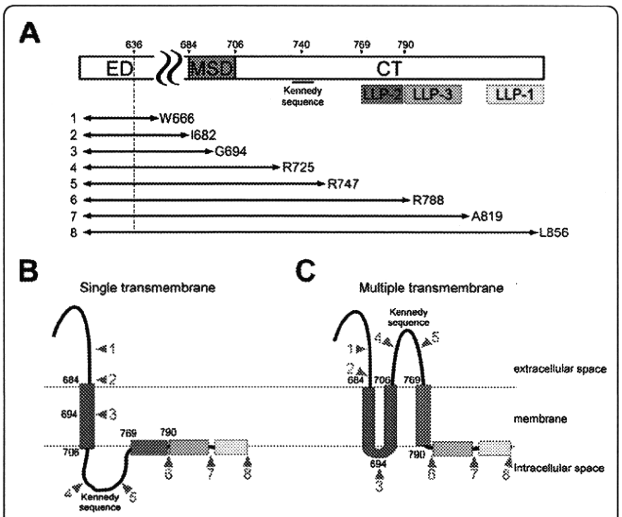

Figure 1 Schematic representation of Env mutants used in this study and the proposed topology models. (A) The points of truncation of gp41 were indicated together with a schematic diagram of the gp41 subunit. ED: ectodomain, MSD: membrane-spanning domain, CT: cytoplasmic tail, LLP: lentiviral lytic peptide. The numbering of the amino acid is based on that of the HXB2 strain. The vertical dashed line shows the position of the N-terminus of the gp41 used for the analysis in the bacterial system. The numbers and letters on the right indicate the position and the amino acid residue of the C-terminus. (B and C) Proposed topology models. The grey numbered arrowheads indicate the truncation points of gp41, the numbers and colors correspond to (A).

gp41 was assigned to the cytoplasmic side of the cellular membrane [11], hence the gp41 subunit is regarded as a type I membrane protein with a single MSD. Other studies provided data consistent with this single MSD model. For example, two cysteine residues for palmitoylation are located in the cytoplasmic domain: one in the middle of LLP-1 (Cys-838) and the other at the upstream of LLP-2 (Cys-765) [12]. The internalization motif, YXXL (Tyr-769 to Leu-772), at the beginning of LLP-2 [13] also maps to the cytoplasmic domain of the single MSD model.

On the other hand, the mapping of the epitopes for neutralizing antibodies called into question the single MSD model. Some of the epitopes were mapped to the cytoplasmic region which contained the amino acid sequence known as the Kennedy sequence (^{724}PRGPD RPEGIEEEGGERDRDRS^{745})[14-16] (Figure 1A). Furthermore, a report using an antibody raised against the LLP-2 portion revealed target binding during membrane fusion when added extracellularly [17]. As antibodies in general are not expected to cross intact membranes, an alternative membrane topology model of gp41 has been suggested in order to assign the mapped epitopes in the extracellular region [16] (Figure 1C). In this alternative model multiple MSDs were proposed because the C-terminus was assumed to be in the cytoplasm. Furthermore, the transmembrane portion of the single MSD model is expected to cross the membrane twice and one of LLPs, LLP2, is a putative third MSD (Figure 1C).

Several studies of the transmembrane portion of the single MSD model showed that it plays a critical role in the modulation of the membrane fusion process, which is an essential step of the HIV-1 life cycle [18-24]. Therefore analysis of the topology and structures of the transmembrane domain of gp41 is critical for our understanding of the mechanism of the membrane fusion. Furthermore the location of the neutralizing epitopes for antibodies is vital for a vaccine development.

In this study we reexamined gp41 topology in two different biological systems; prokaryotic and mammalian systems. The results of prokaryotic and mammalian systems without membrane fusion supported the single MSD model. The results obtained in the mammalian system in the presence of membrane fusion seem to support a transient alteration of the membrane topology of gp41. It is important, however, to note that the effect of the induction of membrane permeability during HIV-1 Env-mediated membrane fusion cannot be excluded. The induction of membrane permeability was reduced by replacing the HIV-1 MSD with that of a foreign protein, CD22.

Methods

Plasmid construction

All PCR amplicons were first cloned into pCR4Blunt-TOPO using the TOPO cloning kit (Invitrogen, Carlsbad, CA) and sequences were verified.

For the topology analysis in the prokaryotic system, the expression vector pKMal-p2e was generated. pKMal-p2e has a kanamycin resistance gene derived from pK18 instead of β-lactamase in the context of pMal-p2e (NEB, Beverly, MA). The oligonucleotide adaptor generated by annealing the following two oligonucleotides: 5'-GTACCG AACAAT TACAC AAGCTTC GGATC CTCTAGA GTCGAC CTGCAG GC G-3' and 5'-AGCTC GC CTGCAG GTCGAC TCTAGA GGATCC GAAGCT TGTGTA ATTGTT CG -3' were inserted into pKMal-p2e to modify the multiple cloning site. This modified vector was named as mpKMal-p2e. The green fluorescent protein (GFP) gene as the reporter for the membrane topology was prepared by PCR using GFPopt$_{1\text{-}11}$ in pCR4Blunt-TOPO [25] as the template with 5'-GAC **TCTAGA** ATGGTG AGCAAG GGCGAG GAGC-3' and 5'-GCA**CTG CAG**TCA GGTGAT GCCGGC GGCGT-3' as the forward and reverse primer, respectively, and cloned into mpKMal-p2e vector using *Xba*I and *Pst*I sites. The generated vector was named as mpKMalp2e-GFP (Table 1).

Table 1 Plasmids used in this study

Plasmids	*Description*
For prokaryotic system	
mpKMalp2e-GFP	Multiple cloning site-modified pMalp2e containing *Kan*^{R} and Green fluorescent protein genes
mpKMalp2e-gp41-1-GFP	mpKMalp2e-GFP with C-terminally truncated gp41 at W666
mpKMalp2e-gp41-2-GFP	mpKMalp2e-GFP with C-terminally truncated gp41 at I682
mpKMalp2e-gp41-3-GFP	mpKMalp2e-GFP with C-terminally truncated gp41 at G694
mpKMalp2e-gp41-4-GFP	mpKMalp2e-GFP with C-terminally truncated gp41 at R725
mpKMalp2e-gp41-5-GFP	mpKMalp2e-GFP with C-terminally truncated gp41 at R747
mpKMalp2e-gp41-6-GFP	mpKMalp2e-GFP with C-terminally truncated gp41 at R788
mpKMalp2e-gp41-7-GFP	mpKMalp2e-GFP with C-terminally truncated gp41 at A819
mpKMalp2e-gp41-8-GFP	mpKMalp2e-GFP with full-length gp41
optGFP$_{1-11}$/pET-47md	Modified pET-47b with modified super folder GFP
For mammalian system	
pHIVenv-Halo	The CMV promoter driven mammalian expression vector containing HaloTag gene
pHIVenv-gp41-4-Halo	pHIVenv-Halo containing Env with C-terminally truncated gp41 at R725
pHIVenv-gp41-5-Halo	pHIVenv-Halo containing Env with C-terminally truncated gp41 at R747
pHIVenv-gp41-6-Halo	pHIVenv-Halo containing Env with C-terminally truncated gp41 at R788
pHIVenv-gp41-7-Halo	pHIVenv-Halo containing Env with C-terminally truncated gp41 at A819
pHIVenv-gp41-8-Halo	pHIVenv-Halo containing full-length Env
pHIVenv-gp41-5	Halo-deleted pHIVenv-gp41-5-Halo
pHIVenv-gp41-8	Halo-deleted pHIVenv-gp41-8-Halo
pHIVenv-CD22-gp41-5	The gp41 MSD replaced pHIVenv-gp41-5 with the MSD of CD22
pHIVenv-CD22-gp41-8	The gp41 MSD replaced pHIVenv-gp41-8 with the MSD of CD22
pHook-Halo-GPI	The expression vector of the GPI anchored-HaloTag
pKcTac-Halo	The expression vector of Tac antigen of IL-2 receptor fused with C-terminal HaloTag
pKcTac-FLAG	pKcTacHalo vector whose HaloTag was replaced with 3xFLAG

This plasmid was used for the negative control for the experiment.

The near full-length gp41 gene derived from the HIV-1 HXB2 strain was amplified by PCR using pGEM7zf(+)-NB [23] as a template with 535fACC651 (Met):5'-AGT**GGT ACC**GAT GACGCT GACGGT ACAGGC CAGA-3' and 856 rXbaI: 5'-GTC**TCT AGA**-TAG CAAAAT CCTTTC CAAGCC CTG-3' as the forward and the reverse primer, respectively. The plasmid that harbors near full-length gp41 in pCR4blunt-TOPO was named as pEnv-HXb2gp41. For the construction of the gp41 mutants, the C-termini were serially truncated, (see Table 1 and Figure 1A), the various gp41 fragments were amplified by PCR using pEnv-HXb2gp41 as a template, with the oligonucleotide 535fACC651 as a forward primer, and the corresponding reverse primer designed for each truncation site. These truncated gp41 fragments were cloned into the vector mpKMalp2e-GFP with *Hin*-*d*III, which is present in the gp41 gene, and *Xba*I at the 5' and 3' terminus, respectively of the fragments. Figure 2A shows the resulting mpKMalp2e-gp41-GFP fusion constructs. The plasmid, optGFP$_{1-11}$/pET-47md [26]

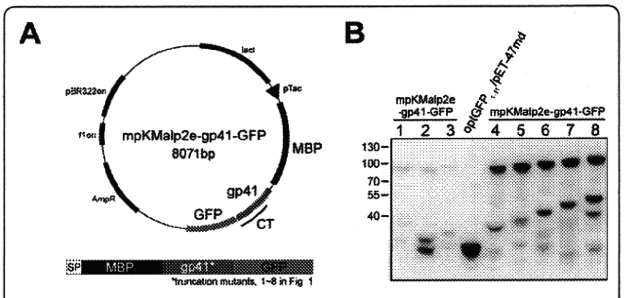

Figure 2 Constructs used to express recombinant gp41 in the *E. coli* system. (A) The expression vectors used in this study. The *env* gene is derived from HIV-1 HXB2 strain. gp41 starts amino acid 636 and ends with the various C-terminal positions as indicated in Fig. 1A. The schema below the plasmid map shows the components of the recombinant proteins. The truncated gp41 is preceded by maltose binding protein (MBP) and followed by the topological reporter, green fluorescent protein (GFP). The nomenclatures are as follows: lacI, lacI repressor gene; pTac, a hybrid promoter between trp and lac promoters; CT, cytoplasmic tail; AmpR, ampicilin resistant gene; f1ori, replication origin of f1; pER322ori, replication origin of pBR322 plasmid. (B) Expression of the recombinant proteins. The immunoblotting of bacterial lysates probed with the anti-GFP antibody is shown. The name on the top of each lane indicates the expression vector used (see Table 1).

that expresses GFP in the cytoplasm was used as a positive control.

The Halo7 gene was amplified by PCR using pFC14k-HaloTag7 (Promega, Madison, WI) as a template, with 5'- **GTCGAC** GGCGGT GGCGGT AGCGGA TCCGAA ATCGGT ACTG-3' and 5'- **GGTACC** TTAACC GGAAAT CTCCAG AG -3' oligonucleotides as the forward and the reverse primer, respectively. The forward primer contained a *Sal*I site and short linker sequence, Gly_4Ser, between the *Sal*I site and Halo7 coding region. The reverse primer included an *Acc65*I site. The amplicon was inserted into the pHIVenvOPT vector, containing an envelope gene based on HXB2 strain that was optimized for human codon usage. The vector generated was named as pHIVenv-Halo (Figure 3A). To construct the truncation gp41 mutants for the mammalian analyses, five different positions were chosen as the C-terminal truncation points (Figure 1A and Table 1). The fragments of truncated *env* from *Xmn*I to each termination codon were amplified by PCR using pHIVenvOPT as a template with 5'-**GCTAGC** AAATTA AGAGAAC-3' including the *Sal*I site as the forward primer and the corresponding oligonucleotides at the truncated sites as the reverse primers, respectively. The *env* fragments were inserted into pHIVenv-Halo (Table 1). For the construction of pHIVenv-gp41-5 and pHIVenv-gp41-8, stop codon-containing oligonucleotides generated by annealing 5'-TCGACTGATGAG -3' with 5'-GTACCTCATCAG-3' was replaced with HaloTag gene to delete HaloTag. The Env expression vector with the MSD of CD22 [27] was constructed using PCR and replacement of the original MSD with the MSD of CD22. As for the control plasmids, two other expression vectors were constructed. The glycosylphosphatidylinositol (GPI)-anchored HaloTag gene was constructed as a marker for surface expression of HaloTag (Halo-GPI in Figure 3A and Table 1). The GPI signal is derived from decay accelerating factor of human origin [28]. A Tac antigen, which is alpha subunit of Interleukin-2 receptor and is a single transmembrane protein [29], was fused with HaloTag gene at the C-terminus (Tac-Halo in Figure 3A and Table 1). This construct was used for the expression of the HaloTag protein in the cytoplasm. A derivative of this expression vector for Tac with a FLAG epitope at its C-terminus (Tac-FLAG) was generated by replacing the HaloTag sequence with that for 3xFLAG tag.

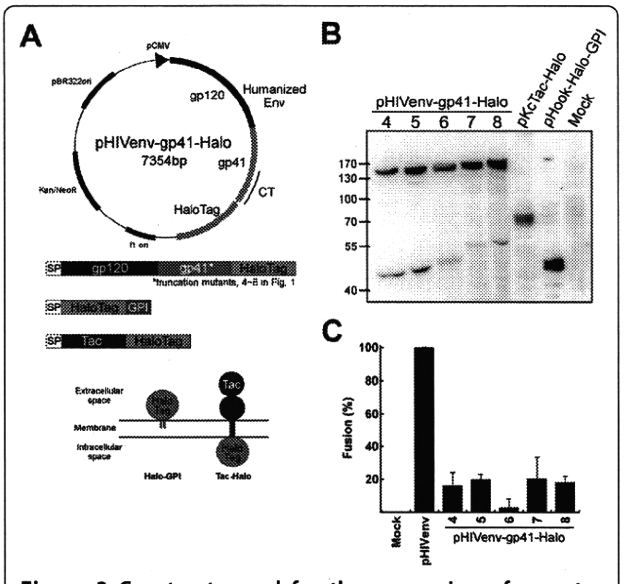

Figure 3 Constructs used for the expression of reporter proteins in the mammalian system. (A) The expression vector used in this study. The *env* gene of HXB2 origin was codon-optimized for human genes. The nomenclatures are as follows: pCMV, cytomegalovirus promoter; CT, cytoplasmic tail; HaloTag, Halo7 gene; f1ori, replication origin of f1; Kan/NeoR, kanamycin or neomycin resistant gene; pER322ori, replication origin of pBR322 plasmid. The composition of the fusion protein used in the study was indicated below the plasmid map. The gp41 proteins with different C-terminal truncation points were fused to HaloTag at their C-terminus. The Halo-GPI, and Tac-Halo constructs and their expected membrane topology are shown schematically. (B) The result of immunoblotting with anti-HaloTag antibody. The names of the mammalian expression vector used are indicated above each lane. (C) Analysis of membrane fusion efficiency. The fusion activity of Halo-fused Env was evaluated by the syncytia-forming activity in 293CD4 cells. The percentage of the number of the nuclei included in syncytia was calculated by counting 300 nuclei in total. The constructs tested are indicated at the bottom of each bar; the number indicated the truncation points shown in Fig.1A.

Expression of GFP-fused gp41 proteins and measurement of GFP fluorescence intensity

E. coli strain BL21 transformed with mpKMal-p2e carrying serially truncated gp41 genes fused to GFP reporter was grown overnight at 22°C in TAG medium (10 g/L Tryptone, 5 g/L NaCl, 5 g/L Glucose, 7 g/L K_2HPO_4, 3 g/L KH_2PO_4, 1 g/L $(NH_4)_2SO_4$, 0.47 g/L Sodium Citrate) with 50 μg/ml kanamycin. The overnight bacterial culture was diluted 1:50 in 4 ml TAG fresh medium containing 50 μg/ml kanamycin and growth was continued at 22°C until the OD_{600} reached 0.2. Cells were grown for overnight in the presence of 0.1 mM IPTG. Subsequently, one ml aliquot of culture was collected and resuspended in 0.5 ml of PBS buffer and the GFP fluorescence intensity was measured by flow cytometry using a FACS Calibur (BD Biosciences, Mississauga, ON). At the same time, another 1 ml aliquot of culture was dispensed for SDS-PAGE and immunoblotting analysis.

Mammalian cell culture, transfection, labeling, and imaging

The 293FT cells (Invitrogen, Carlsbad, USA) or 293CD4 cells (293 cells constitutively expressing human CD4) [23]

were grown in 96-well Matriplates (GE Healthcare, Piscataway, NJ) with Dulbecco's modified Eagle medium (DMEM; Sigma, St. Louis, USA) supplemented with 10% FBS (Hyclone Labs., Logan, UT). In the case of 293FT, 5 μg/ml Geneticine (GiBco, Grand Island, USA) was further supplied. Cells were grown at 37°C in 5% CO_2 incubator.

DNA transfection of mammalian cells was performed using Fugene HD (Roche, Indianapolis, USA; Fugene HD (μl): DNA(μg): DMEM(μl) = 5:2:200). The transfection mix was incubated for 15 mins at room temperature prior to addition to the cell culture in a drop-wise manner (10 μl per well). After certain hours of transfection the transfected cells were subjected for further analyses as described below.

At the indicated time after transfection, the transfected cells were probed with HaloTag ligands. The starting time point of labeling after transfection was different for different experiments involving a different set of cells and vectors (see the Results section). The labeling was performed as suggested by the manufacturer (Promega). Briefly, the transfected live cells were labeled for 15 mins at 37°C with 1 μM of HaloTag ligand Alexa Fluor 488 (AF488), a membrane-impermeable ligand, or Oregon Green (OG), a membrane permeable ligand, respectively. After labeling, the cells were rinsed three times with 200 μl prewarmed DMEM plus 10% FBS and subsequently incubated at 37°C with 5% CO_2 for 30 mins. The medium was changed with fresh warm DMEM plus 10% FBS, then images were captured using a confocal microscope (Olympus FluoView FV1000, Tokyo, Japan).

Immunofluorescent staining assay using the anti-FLAG monoclonal antibody (Sigma) was performed to detect the FLAG-tagged proteins as below. Following the fixation of the transfected cells with 2% paraformaldehyde at 25°C for 5 mins, the anti-FLAG antibody (1/200 in 0.5% BSA and PBS) was used as the first antibody. After incubating at room temperature for 1 h, the cells were rinsed 3 times with 200 μl prewarmed PBS plus 0.5% BSA and subsequently incubated with anti-mouse antibody conjugated with AlexaFluor 488 (Invitrogen) (1/200 in 0.5% BSA and PBS) at room temperature for 1 h. The images were captured using a confocal microscope (Olympus).

To evaluate the cell viability, staining with propidium iodide (PI) [30] was used. In the case of co-labeling with the HaloTag ligands, staining with AF488 was performed first, then PI staining for 15 min at room temperature with a final concentration of 2.5μg/ml followed. The cells were rinsed two times with PBS and images were analyzed as described above. In the case of co-staining with anti-FLAG monoclonal antibodies, PI staining was performed first, followed by labeling with the anti-FLAG monoclonal antibody.

To mimic the effect of the conformational changes of gp120 after its binding to the CD4 receptor, soluble CD4 was added to the 293FT cells transfected with HIV-1 Env expression vectors. The soluble CD4 protein (final concentration: 0.1 μM) was kept in the medium since immediately after transfection.

Syncytia formation assay

A syncytia formation assay was performed by transfecting the HIV-1 Env expression vectors (listed as For mammalian system in Table 1) into the 293CD4 cells. The cells were transfected when they were about 50% confluent. At 48 h after transfection, the images were captured with IN Cell analyzer 1000 (GE Healthcare, Uppsala, Sweden). The fusion activity of Halo-fused Env was evaluated by counting 300 nuclei in total after staining with 2 μM Hoechst and determining the percentage of nuclei included in syncytia.

Immunoblot analysis

Bacterial cultures (1 ml) were harvested and resuspended in 50 μl SDS-PAGE loading buffer (2% SDS, 2 mM DTT, 10% glycerol, 50 mM Tris-HCl, pH6.8, 0.01% Bromo phenol blue). The mixture was kept for 10 mins at 95°C and subjected to centrifugation (20,000 g, 4°C) with MX-301 (Tomy, Japan) to remove the pellets. Whole cell lysates (2 μl) were resolved using a 5-20% gradient SDS polyacrylamide gel (DRC, Tokyo, Japan). The proteins were transferred to the PVDF membrane and probed with 15,000-fold diluted anti-GFP antibody (Santa Cruz Biotechnology, Santa Cruz, USA) for 1 h at room temperature. Anti-mouse antibody (GE healthcare), diluted by 5,000-fold, was used as the secondary antibody. The signal was developed by streptavidin-biotinylated horseradish peroxidase complex (GE healthcare) and the chemiluminescence reagents (Roche), and detected by LAS3000 (Fuji).

The transfected 293FT cells grown in 10-cm dishes as described above were collected and centrifugated (5,000 g, 4°C) with MX-301. The cell pellet was lysed with 250μl of RIPA lysis buffer [50 mM Tris-Cl (pH 7.4), 150 mM NaCl, 1% NP-40, 0.1% SDS] and then centrifuged (MLA-130 rotor, 100,000rpm, 30 mins, 4°C) with Beckman Optima™Max Ultracentrifuge. The supernatant (20 μl) was treated with the same method as described above. The protein bands on the PVDF membrane were developed as described above, except for the 500-fold diluted anti-Halo pAb (Promega) and 5000-fold diluted anti-rabbit antibody (GE healthcare) which were used as the primary and secondary antibodies, respectively.

Results

Topology mapping of gp41 using GFP as a reporter in a prokaryotic system

We first employed the well-established prokaryotic topological analysis using GFP as a reporter [31,32]. If

GFP is located in the cytoplasm it folds into an active form, whereas when it is translocated into the periplasm it is non-functional [31]. The periplasm-targeted maltose-binding protein was placed at the N-terminus of the gp41 portion to be tested, and then GFP, a topological reporter, was fused to the C-terminus of the gp41 fragment (Figure 2A). The series of gp41 proteins truncated at the different C-terminal positions were tested (Figure 1A and Table 1). The N-terminus of gp41 portion included was fixed at the position of 636th amino acid close to the predicted MSD (Figure 1A dotted line), because there is little controversy on the beginning of the MSD itself.

After transformation of *E. coli.* with one of the plasmids, the expression of the recombinant protein was evaluated by immunoblotting using an anti-GFP antibody and the results are shown in Figure 2B. The levels of protein expression with mpKMalp2e-gp41-1-GFP, mpKMalp2e-gp41-2-GFP, and mpKMalp2e-gp41-3-GFP, were low (Figure 2B), and we did not analyze these constructs further. The rest of constructs each expressed a comparable amount of the fusion protein of about 100kD (Figure 2B). The fluorescence intensities of GFP at 530 nm of *E. coli* induced for the expression of the fusion proteins were measured by a flow cytometry. Compared with the negative control that expresses GFP in the periplasm (mpKmalp2e-GFP), the GFP intensity adjusted by the cell density was significantly higher for mpKMalp2e-gp41-4-GFP, mpKMalp2e-gp41-5-GFP, mpKMalp2e-gp41-6-GFP mpKMalp2e-gp41-7-GFP and mpKMalp2e-gp41-8-GFP (Table 2). This suggested that GFP attached at the position 4 to 8 lies in the cytoplasm. Interestingly, there was no significant difference in the GFP fluorescent intensity adjusted by the level of the expression for mpKMalp2e-gp41-4-GFP, mpKMalp2e-gp41-5-GFP, mpKMalp2e-gp41-6-GFP, mpKMalp2e-gp41-7-GFP and mpKMalp2e-gp41-8-GFP. These data suggested that there was no topological shift of GFP reporter in these regions; therefore the Kennedy sequence and LLP regions are not exposed to the periplasmic region. These results are consistent with the single MSD model of gp41 (Figure 1B).

Table 2 Results of GFP quantification

Vector	Adjusted GFP signal (The number of counts /OD_{600})
$optGFP_{1-11}$/pET-47md	4026.238
mpKMalp2e-gp41-4-GFP	1103.775
mpKMalp2e-gp41-5-GFP	971.453
mpKMalp2e-gp41-6-GFP	828.177
mpKMalp2e-gp41-7-GFP	1018.790
mpKMalp2e-gp41-8-GFP	986.997
mpKmalp2e-GFP	313.958

Expression of HaloTag-attached HIV-1 Env in mammalian cells

Although the bacterial system is quick and informative, eukaryote specific post-translational modifications and/or the difference in the composition of lipids in the membrane may affect the topology of gp41. Therefore, HIV-1 Env with the C-terminus of gp41 linked to HaloTag was expressed in mammalian cells (Figure 3A). The HaloTag is a 33 kDa protein designed to covalently bind to its membrane-permeable/impermeable ligands conjugated with a fluorescent chromophore [33]. Based on the previous published results [11] and our own results of the prokaryotic system (see above), we focused on the analysis of the region after the predicted MSD of the single MSD model (truncation positions 4-8 in Figure 1A). The GPI-anchored HaloTag protein (Halo-GPI) and the HaloTag attached to the C-terminus of the Tac antigen after MSD (Tac-Halo) were made as the controls for the extracellular and intracellular positioning of HaloTags, respectively (Figure 3A and Table 1). Expression of HaloTag-attached envelope proteins was confirmed by immunofluorescence analysis with anti-gp120 antibody (data not shown) and immunoblotting analysis with anti-Halo antibodies (Figure 3B). The bands around 130-170kD and 40-55kD for pHIVenv-gp41-Halo are HaloTag-attached gp160 and gp41, respectively.

The membrane fusion capacity of these mutants was examined with a syncytia formation assay by transfecting the expression vector into 293CD4 cells [23]. Although the efficiency of the fusion was reduced in all of the HaloTag-attached envelope proteins, all still retained membrane fusion activity (Figure 3C). When we analyzed the fusion activity with the DSP assay [34], better fusion was observed (data not shown). Since the DSP assay relies on the smaller reporter proteins, the presence of the defect of pore dilatation in HaloTag attached mutants was suggested.

Topology mapping of gp41 in mammalian cells using HaloTag-specific membrane-impermeable ligands

The membrane-permeable and membrane-impermeable ligands with fluorescent chromophore available for HaloTag were used to examine the location of the attached HaloTag in relation to the cell membrane. Oregon Green (OG) that readily cross the cell membrane labels HaloTag located in both extracellular and intracellular spaces, whereas Alexa Fluor 488 (AF488), a membrane-impermeable ligand, should label HaloTag exposed on the cell surface. When we used the membrane-permeable substrate, OG, all of the 293FT cells transfected with HaloTag-fused truncated Env

plasmids (pHIVenv-gp41-4-Halo, pHIVenv-gp41-5-Halo, pHIVenv-gp41-6-Halo, pHIVenv-gp41-7-Halo, and pHIVenv-gp41-8-Halo) were stained by the ligand (Additional File 1; Figure S1). The 293FT cells transfected with pHook-Halo-GPI and pKcTac-Halo were also stained by OG; the fluorescent signal was localized at the rim of the cells (Additional File 1; Figure S1). On the other hand, when we used the membrane-impermeable substrate, AF488, none of the 293FT cells transfected with the plasmids harboring HaloTag-fused Env with C-terminal truncation were stained (Figure 4 pHIVenv-gp41-4 to -8-Halo). As expected, the 293FT cells transfected with pHook-Halo-GPI were stained by AF488, but the 293FT cells transfected with pKcTac-Halo did not show any fluorescent signal under the same labeling and imaging conditions (Figure 4), verifying the authenticity of this experimental system. These results indicate that the HaloTag attached at positions 4 to 8 of gp41 are located in the cytoplasm of the cells. This result is consistent with the prokaryotic data (Table 2) and suggests that Kennedy sequence and LLP regions are both located in the cytoplasm, supporting the single MSD model of gp41 [11].

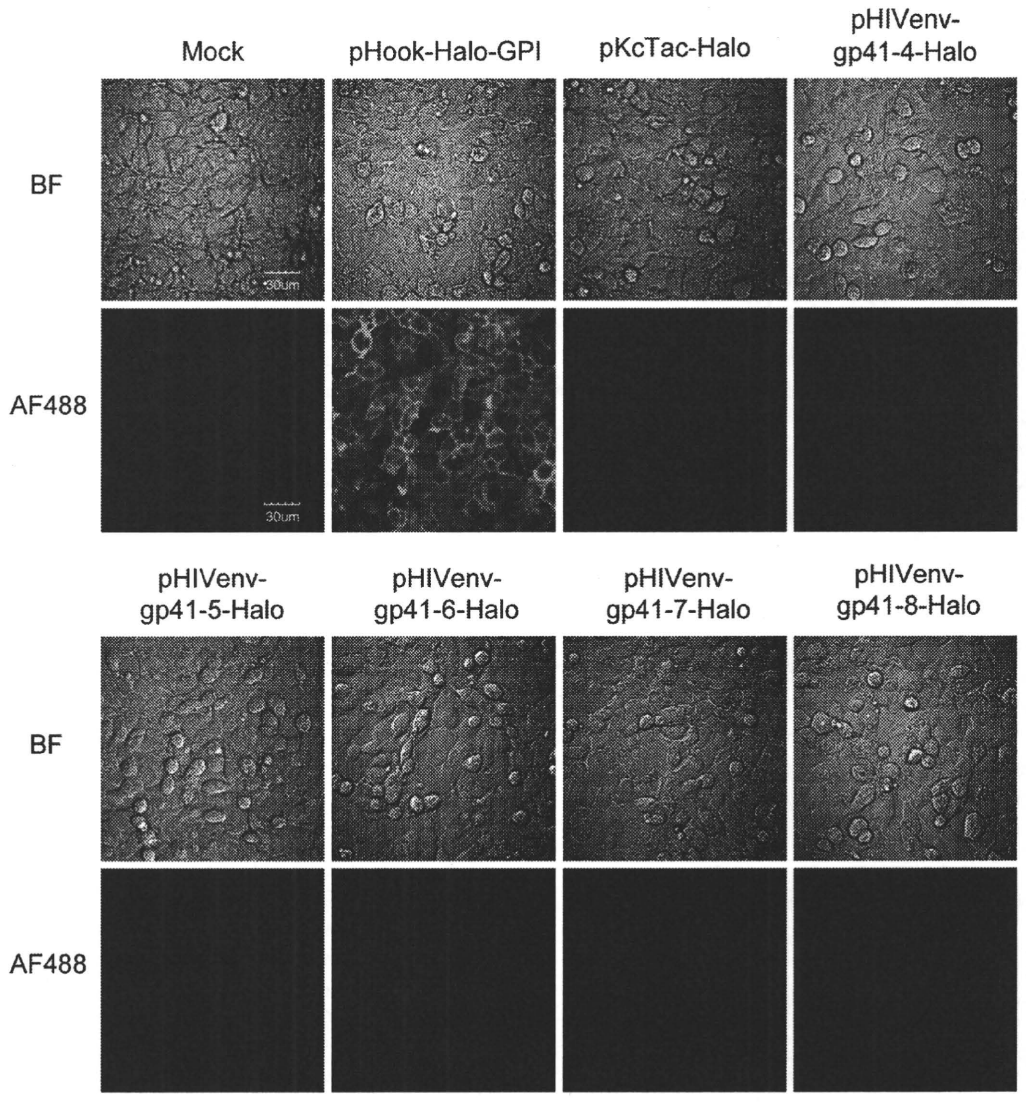

Figure 4 Topological analysis of gp41 in 293FT cells. Images of the cells stained with the membrane impermeable ligand, Alexa Fluor 488 (AF488), for HaloTag. The staining and image capturing were done at 44 h post transfection. Mock, mock DNA transfection. The names of expression vectors are shown. The bar indicates 30 μm.

Examination of membrane topology with HaloTag in syncytia formed in 293CD4

As the possibility for a transient topological change of gp41 during membrane fusion has been proposed [16,17], we induced the formation of syncytia in 293CD4 by transfecting a series of Env-HaloTag expression vectors and performed the labeling. All of the syncytia formed after transfecting the expression vector for each Env-HaloTag were positively stained with OG, membrane-permeable ligand, during membrane fusion, confirming the expression of Halo-fused Envs (Additional File 2; Figure S2). When the membrane-impermeable ligand AF488 was used for staining, most of the multinucleated 293CD4 cells expressing various gp41 truncation mutants were not stained (Figure 5). The only exception was the cells transfected with pHIVenv-gp41-5-Halo, in which rare and weak staining of the syncytia were observed (Figure 5). Even the later time points with the similar levels of syncytia formation with pHIVenv-gp41-8-Halo were chosen to compensate the reduced fusion efficiency of pHIVenv-gp41-5-Halo, the staining incidence for pHIVenv-gp41-5-Halo did not increase. The 293CD4 cells transfected with the control plasmids, pHook-Halo-GPI (HaloTag on the cell surface) and pKcTac-Halo (HaloTag in the cytoplasm), showed the results consistent with their expected topological locations (Figure 5 pHook-Halo-GPI and pKcTac-Halo).

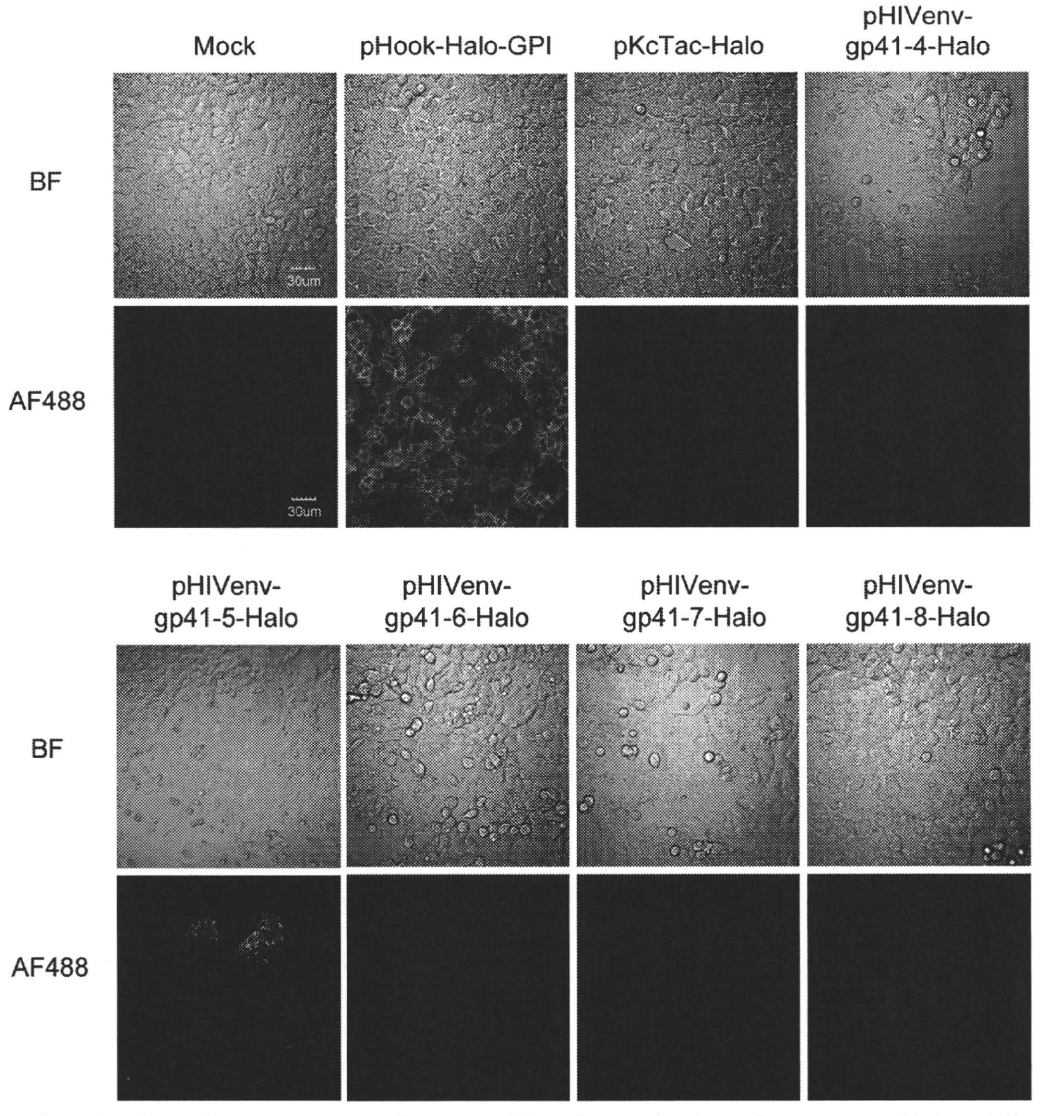

Figure 5 Topological analysis of gp41 in 293CD4 cells. Images of the cells stained with membrane impermeable ligand, Alexa Fluor 488 (AF488). The staining and image capturing were done at 20 h post transfection. The abbreviations used are same as in Fig. 4. The bar indicates 30 μm.

When the 293CD4 cells transfected with pHIVenv-gp41-5-Halo were stained with the anti-HaloTag antibody without permeabilization procedure, rare events of staining were observed (data not shown). These results suggest that the possibility of sporadic exposure of cytoplasmic domain of gp41 during membrane fusion with pHIVenv-gp41-5-Halo.

Augmented membrane permeability by Env-induced membrane fusion

The result shown above for pHIVenv-gp41-5-Halo could be an indication of a rare translocation of the cytoplasmic region of the gp41. The reason why the translocation, if happening, is limited to the truncation at position 5 with a very low incidence was not clear. Since there was no staining for pHIVenv-gp41-4-Halo, we have to assume a hypothetical MSD between the position 4 and 5. This is to assume the Kennedy region to be the hypothetical MSD and is different from the model shown in Figure 1C. The hydrophilic Kennedy sequence is not likely to be an MSD by several prediction algorithms (Table 3). An alternative possibility is that the sporadic staining was due to the induced permeability of membranes in syncytia.

To distinguish the alteration of gp41 topology from membrane permeability induced during membrane fusion, we co-expressed tag-free HIV-1 Env together with Tac-Halo in the same cells. Namely, the pKcTac-Halo, and pHIVenv-gp41-5/pHIVenv-gp41-8 or pHIVenv-CD22-gp41-5/pHIVenv-CD22-gp41-8 (Table 1) were co-transfected simultaneously. We then probed the HaloTag expressed in the cytoplasmic side (see Figure 3A) with AF488, membrane-impermeable ligands. Both 293FT (fusion incompetent) and 293CD4 (fusion competent) cells were used to determine the effect of membrane fusion. The co-transfected 293FT cells were not stained with AF488 (Figure 6 -soluble CD4), whereas these cells were stained with OG (data not shown). The expressions of Env in 293FT cells were confirmed by immunoblotting (Additional file 3; Figure S3). The addition of soluble CD4, which can induce the early conformational change of gp120, did not show any changes in the staining patterns (Figure 6 + soluble CD4).

Table 3 Computational analyses of possible transmembrane domain

Program	Region of the predicted membrane-spanning segment (original: 684-706)
TroPred	684-705
TMHMM	678-701
SOSUI_MP1	675-708
SOSUI	683-706

In the case of 293CD4 cells, however, the co-transfected cells (Figure 7 -C34, pHIVenv-gp41-5 or 8 + pKcTac-Halo,) could be clearly stained by AF488 at the site of syncytium (Figure 7 -C34). These staining were not due to the cell death, because some cells labeled with AF488 did not show the staining with propidium iodide (Figure 7 shown in red). The staining with AF488 was abolished when membrane fusion was inhibited by the addition of C34, an inhibitor of six-helix bundle formation (Figure 7 +C34, pHIVenv-gp41-5 or -8 +pKcTac-Halo). These results indicated that the induction of the permeability was dependent on active membrane fusion.

To examine whether the observed membrane permeability during membrane fusion allows antibodies to penetrate membranes, we probed the 3 × FLAG epitope attached to the cytoplasmic portion of the Tac antigen (Tac-FLAG) with the anti-FLAG antibody. The intracellular 3 × FLAG tag was detectable when HIV-1 Env with or without the truncation, pHIVenv-gp41-5 and pHIVenv-gp41-8, respectively, were co-expressed (Figure 8 -C34). Although the staining pattern of each syncytium varies, it seemed that the incidence of the positively stained syncytia was slightly lower than that obtained with the membrane-impermeable ligands shown in Figure 7. When the membrane was permeabilized with detergent prior to antibody staining, all of syncytia were stained well (data not shown). These results suggest both the full-length and truncated Env have the ability to permeabilize the membrane to allow the antibodies to cross the membranes.

Augmented membrane permeability is dependent on MSD sequence

Since membrane permeability was induced in the cells transfected with pHIVenv-gp41-5-Halo, the presence of LLPs is not required for the increased permeability. To further characterize the region required for this enhanced permeability we constructed the mutants in which the original gp41 MSD was replaced with the foreign MSD derived from CD22 [27] in the pHIVenv context. Previous reports indicated that the MSD derived from CD22 did not alter the function of HIV-1 Env [27]; however, the replacement seemed to delay the appearance of syncytia when compared with the wild type (see below). We compared these mutants with the HIV-1 Env with the native MSD. In the case of the HIV-1 Env with its native MSD, intracellular HaloTag was detectable with membrane-impermeable AF488 at the earlier time point after co-transfection (16 h post transfection, Figure 7; pHIVenv- gp41-5 and 8). On the other hand, there was minimal staining in cells co-transfected with HIV-1 Env with CD22 MSD at 16 h after transfection (data not shown). At 44 h post transfection when the cells transfected with the native gp41 MSD were almost gone due to

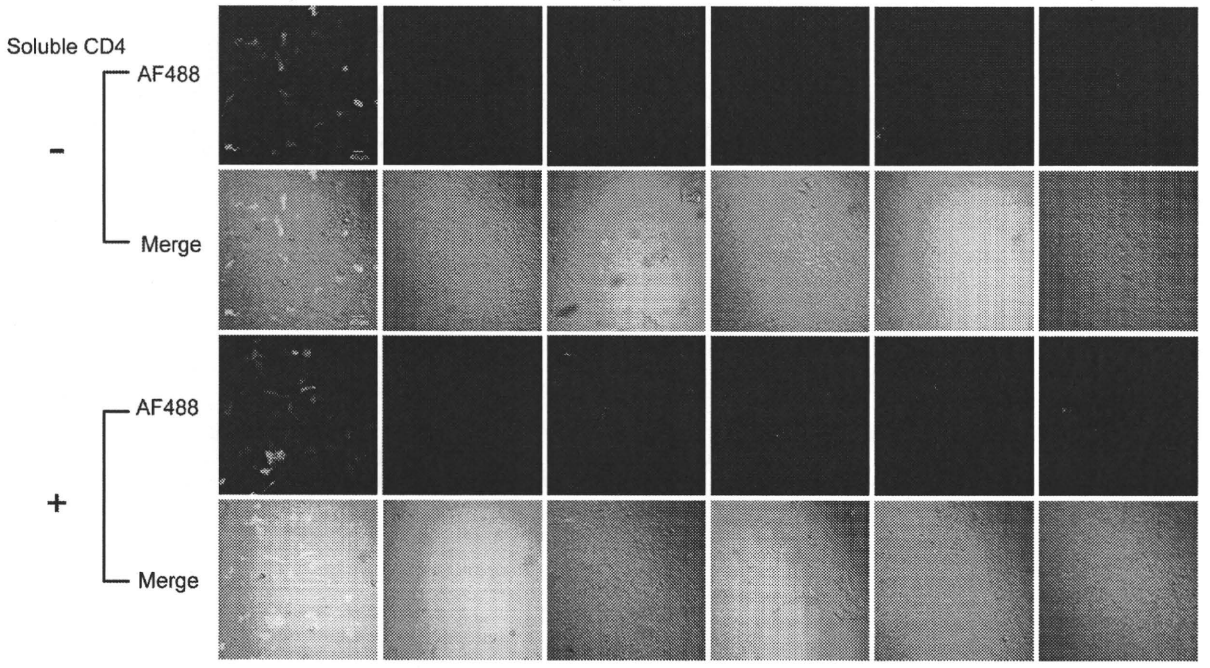

Figure 6 Staining of 293FT cells cotransfected with the Env expression vector and pKcTac-Halo in the presence or absence of soluble CD4 by membrane-impermeable ligand, Alexa Fluor 488 (AF488). Soluble CD4 (0.1 μM) was used to induce the conformational changes of gp120. The names of the expression vectors used were shown on top. Merge: merged images of bright field and AF488 signals. The bar indicates 40 μm.

the cell death, some cells transfected with CD22 MSD mutants were stainable with AF488 (Figure 7 -C34, pHIVenv-CD22-gp41-5 or 8 + pKcTac-Halo). Therefore there is a significant difference in the pattern of the staining between the native and CD22 MSDs. At 44 h post transfection, there were more dead cells as indicated by the positive PI staining. These cells were also stained with AF488. There are, however, some syncytia stained only with AF488 for CD22 MSD mutants (Figure 7). Inhibition of the membrane fusion with C34 blocked the staining (Figure 7 +C34). Similar results were obtained if anti-FLAG antibodies were used to detect the FLAG tag located in the cytoplasm. (Figure 8 pHIVenv-CD22-gp41-5 or 8 + pKcTac-FLAG). Taken together, these results indicated that the induction of permeability was membrane fusion-dependent and that the gp41 MSD played some role in the degree of induced permeabilization during membrane fusion.

Discussion

In this study we examined the membrane topology of the gp41 subunit in two different biological systems. The truncated gp41 subunit was tagged with the topological reporter protein at the C-terminus (Figure 1, 2, 3). A prokaryotic reporter, GFP [31,32] and mammalian reporter, HaloTag [33], were used. Both reporters enabled us to examine the topology in living cells without the artifacts caused by fixing.

In our prokaryotic system, all of the tested constructs (mpKMalp2e-gp41-4, 5, 6, 7- and 8-GFP) showed stronger GFP fluorescence than the control. This suggested that gp41 had a single MSD that places the Kennedy sequence, LLP-2, LLP-3, LLP-1 and the C-terminus of gp41 in the cytoplasmic side. The analysis with β-lactamase, another topology reporter, which is only active in periplasm produced the data consistent with that of GFP (data not shown). These data are consistent with the results obtained by the currently available several programs for prediction of transmembrane domains (Table 3).

Our analysis of gp41 topology in mammalian cells without membrane fusion (293FT cells) supported the single transmembrane model, concordant with that of

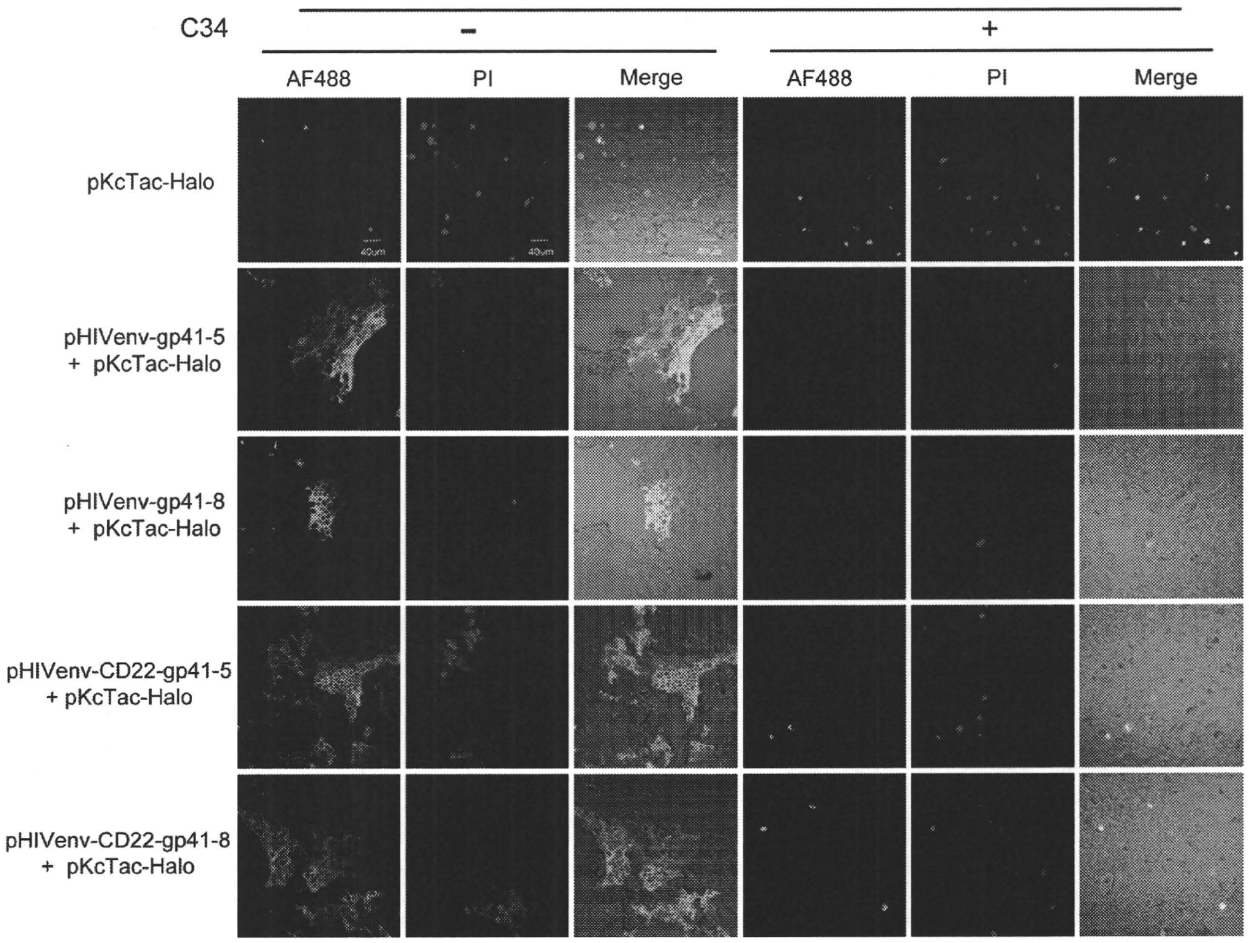

Figure 7 Examination of the membrane permeability during membrane fusion. Staining of 293CD4 cells cotransfected with the Env expression vector and pKcTac-Halo with membrane-impermeable ligand, Alexa Fluor 488 (AF488, shown in green) in the presence (+) or absence (-) of the fusion inhibitor, C34 (2 μM). The names of the expression vectors used are shown in left. Staining and image capturing were performed as described in Methods. For the HIV-1 Env with its native MSD images were captured at 16 h post transfection. The similar assay was performed for CD22MSD mutants at 44 h post transfection. PI: images with propidium iodide staining as described in Methods. Merge: merged images of bright field with AF488 and PI labelings. The bar indicates 40 μm.

the prokaryotic system. Only sporadic staining with membrane impermeable ligands was observed for pHIVenv-gp41-5-Halo (truncation at position 747 in HXB2 Env) in fusion-competent 293CD4 cells. Since staining for the preceding truncation point, pHIVenv-gp41-4-Halo (truncation at the residue 725 in HXB2), was negative, suggesting an additional MSD between the residue 725 and 747. This region contains about 20 mainly hydrophilic amino acid residues that correspond to the Kennedy sequence. As shown in Table 3 no MSD was predicted in this region by several computational algorithms. So we speculated that there is other reason for the observed apparently contradictory observations.

We examined the possibility of enhanced membrane permeability to account for the staining of putative intracellular regions during membrane fusion. The intracellularly located HaloTag was labeled using the membrane-impermeable ligand for HaloTag when HIV-1 Env-mediated membrane fusion occurred (Figure 7). Antibodies were also able to stain the intracellular targets in conditions of membrane fusion (Figure 8). Although we cannot completely exclude the possible alternations of the gp41 topology, the multiple MSD model based on the epitope mapping [16,17] needs to be reevaluated carefully given the increased permeability we have observed.

We attempted to map the region(s) of gp41 responsible for increased membrane permeability. Our data suggested that the increased permeability was dependent on active membrane fusion (Figure 7 and 8). It is consistent with several reports of the fusion-dependent induction of membrane permeability in HIV-1 infected cells [35-38].